

1 Slip deficit and time clustering along the Dead Sea fault from
2 paleoseismological investigations

3

4 Marthe Lefevre (1), Yann Klinger (1), Mahmoud Al-Qaryouti (2), Maryline Le Béon
5 (3), Khaled Moumani (4)

6

7 (1) Institut de Physique du Globe de Paris, Paris, France,

8 (2) Jordan Seismological Observatory, Ministry of Energy and Mineral Resources, Amman,
9 Jordan,

10 (3) Department of Earth Sciences - National Central University, Taiwan,

11 (4) Geological Mapping Division, Ministry of Energy and Mineral Resources, Amman,
12 Jordan.

13

14

15 **Supplementary materials**

16

17 Table of content:

18

| | | |
|----|--|----|
| 19 | 1. Units and fault zone descriptions | 1 |
| 20 | 2. Description of earthquakes ruptures | 4 |
| 21 | 3. Timing of events and Identification of historical earthquakes | 6 |
| 22 | 4. Earthquake catalogue | 14 |
| 23 | 5. Alternative scenarios | 20 |
| 24 | 6. Probability computation | 22 |
| 25 | 7. References | 23 |
| 26 | 8. Table and figures | 27 |

27

28 These supplementary materials consist only in technical descriptions and each part can
29 be read independently of the others.

30

31 **1. Units and fault zone descriptions**

32

33 The trench is about 20 m long and 2.5 m deep. We can distinguish four main units,
34 characteristic of different depositional environments (Fig. 1, Fig. S2). Each unit consists
35 in a series of individual layers. The different strata consist in medium to coarse sand
36 with few clasts and silts. The thickness of the layers varies from a couple of centimeters

37 to a few decimeters. The units tend to be more homogeneous and finer in the upper part,
38 while sediments become coarser and more discontinuous in the lower part.

39 The central unit between marks 3 and 9 (M3-M9) is a reddish unstratified indurated
40 sandy unit with gravels aligned vertically along fault zones (unit A, Fig. S3). This unit (A)
41 has a structure similar to the one of the small push up located a hundred meters to the
42 south of our trench and that brought reddish gravelly sand to the surface (Fig S1). In our
43 trench, however, this structure has been partly eroded and does not reach the surface.

44 At the base of the trench there is a coarse unit (unit B), which contains two layers B1
45 and B2. The lowest layer (B1) consists of a conglomerate of matrix-supported pebbles,
46 overlaid by a layer of indurated fine to medium yellow sand including some thin
47 indurated clayey beds and gravels (B2). The conglomerate (B1) is not continuous
48 laterally: it is visible only between marks M17 and M19, between M12 and M9 and at
49 M2. Layer (B1) is thicker East of unit A, with a triangular shape thinning out eastward
50 and unit A partly overthrusting on layer (B1). Although no obvious bedding could be
51 seen in layer (B1), the compressional nature of unit A suggests that part of layer (B1)
52 was dragged upward during successive activations of the push-up.

53 The unit Cu1 is characterized by channels, some of them flowing perpendicular to the
54 trench, as shown by the lens shape of the gravel beds. The thickness of this unit varies
55 across the trench exposure, to become thinner west of unit A. This variation may be due
56 to the fact that water coming from the Jordan plateau is deflected by the local
57 topographic barrier created by the unit A. The numerous channels in this unit are
58 characteristic of an environment with significant precipitation and dynamic water flow,
59 which could be associated to one of the major wet phases of the Holocene in ~ 5.6–3.5
60 cal kyr BP¹.

61 The upper 1.3 meters of the trench are formed by a series of sub-horizontal laminated
62 sandy layers, beige to dark brown in color. Most of these units can be followed across
63 the trench. These layers are labeled C to layer M (fig S2-S3).

64 Layers C to E are visible only on the eastern part of the trench. C is a thin layer of
65 homogeneous brown sand, more humid than the surrounding units. Layer D is more
66 heterogeneous, as it contains small lenses of gravels in the sand. Layer E is light beige
67 and made of fine sand. Top of layers C-E is characterized by an erosional surface. Units
68 Cu2 directly above this contact show local interfingering with coarser channel material
69 in the middle of the trench (M9-13). This unit is made of finer material and becomes
70 sub-horizontal in the eastern end of the trench. In some place we can distinguish three
71 sub-layers in this unit (M16-17) but there are not continuous, and we consider them as
72 one single unit. As for layers C to E, this unit is not visible in the western part of the
73 trench. The layer F is a 10 cm-thick laminated beige layer. It is made of fine sand and few
74 scattered gravels. The Layer G is a laminated coarse sandy layer. This layer is coarser on

75 the eastern part with gravels and pebbles and shows finer material in the central part
76 (M9-16). On the western part of the trench this layer is thicker and it contains finer
77 laminated sand. On top of G sits the layer H with an erosional contact between G and H.
78 Layer H is brown in color, composed of sand with a large amount of coarse gravels. The
79 layer I is a brown bedded sandy layer including laminas of clayish material white to dark
80 brown in color. Layer J is a fine yellow sandy layer, which can be followed across the
81 trench, although it gets thinner and discontinuous between M17 and M3. A thin
82 discontinuous coarse layer characterized by small gravel lenses erodes into this layer.
83 These lenses form the base of a thick beige laminated sandy layer, the layer K. This layer
84 is well visible in the eastern part of the trench, but seems to be interrupted westward at
85 M9. It is difficult to determine with certainty if it continues further west because of the
86 lateral variation of facies. However, stratigraphic relations argue for a continuation of
87 layer K between M1-M9. Indeed, the lower unit J is visible but discontinuous between
88 M1 and M9, just below a thick unit coarser than the unit K on the eastern part. This
89 coarser unit could be the continuation of layer K, acknowledging some lateral variation
90 of facies that could be due in part to strike-slip motion along faults in a direction
91 perpendicular to the trench. The lack of datable material in the eastern part of layer K
92 prevented us from testing further lateral continuity of the units. At M9 units F to L are all
93 affected by the fault zone, with the western side going down. A channel is nested at the
94 toe of the scarp, which erodes into unit K between M9 and M3. This brown to dark
95 brown channel unit (Cu3) shows large gravel lenses cross-bedded with sandy and more
96 clayish beds. The layers L and M are the only traceable layers across the entire trench.
97 The layer L is a laminated sandy layer containing few pebbles and gravel lenses. Its
98 thickness decreases westward. This layer is erosive into layer K. The layer M is a fine to
99 coarse sandy layer. It contains pebbles and small gravel lenses and clayey beds. In the
100 western section few desiccation figures are visible.

101 The deformation is distributed over 15 m, with two main zones where it is larger. On the
102 western end, between M3 and M9, faulting is mainly associated to the push-up structure
103 formed by unit A. Cracks and fissures show opposite dip on each side of this structure.
104 On the western side of this structure, faults are almost vertical with a slight dip
105 eastward consistent with some minor thrust component of motion related to the push-
106 up structure, in addition to dominant strike-slip faulting. On the eastern side of unit A,
107 faults have a shallower westward dip. Although the stratigraphic position of unit A
108 above unit B suggests that at some point these faults did accommodate some reverse
109 motion in addition to strike-slip, according to obvious offset layers from layer C upward,
110 these faults have mostly accommodated normal faulting during recent activation, in
111 addition to the strike-slip. This motion is consistent with motion accommodated in the
112 second main fault zone located between M16 and M18. In this fault zone, faults and

113 cracks dip westward with an average dip of 60°. In addition to strike-slip, these faults
114 are responsible for down dropping the western part of the trench relative to the eastern
115 part. The vertical motion mostly concentrates at M10 with at least about 30 cm of
116 vertical displacement since 2000 years if we use unit F as a reference. This results in
117 part in thickening of units westward.

118 As often, strike-slip motion is hardly recognizable in a fault-perpendicular trench as it
119 results mainly in abrupt facies or thickness changes due to lateral motion. In our case, as
120 our trench is located in quite an extensive bajada, these changes are even more difficult
121 to see.

122

123 2. Description of earthquakes ruptures

124

125 The identification of earthquake ruptures is mostly based on consistent upward
126 terminations of sets of cracks that vertically offset sedimentary units². It follows the
127 assumption that earthquakes ruptured the surface, thus we focus only on the large
128 events. In the Wadi Araba the locking depth is estimated to be around 12 km^{3,4}.
129 Following the scaling laws of Wells & Coppersmith⁵, event of magnitude 6.6 or above
130 will break the entire brittle crust, which is comparable to the commonly used value of
131 $M_w=6.5^2$. Some smaller events could also be recorded in the trench, if they occurred
132 close to the surface. For the coarser units, like conglomerates, it is particularly difficult
133 to identify the exact location of some cracks termination. However, as coarser units are
134 mostly located at the base of the trench, we consider that we recorded well the major
135 events in the trench, at least for the most recent ones.

136 Eleven events have been unambiguously identified in our trench, and one additional
137 event E5 is less constrained as it is associated to only 4 cracks (Fig S2). The older events,
138 E9 to E11, are observed in the coarsest layers, which present erosive limits, thus
139 deformation associated to these events in the trench is less pronounced than for more
140 recent events. E11 is associated with cracks in the western part of the conglomerate
141 (B1). As the contact with the layer deposited on top of it is erosive, we cannot see any
142 vertical displacement, but cracks are well marked and underlined by rotated vertical
143 pebbles. The presence of an erosive contact implies larger uncertainties on the age of
144 this event, as the actual upper termination of cracks is unknown.

145 The event horizon associated to E10 is located on the top of layer B2. The evidence for
146 this event is largely distributed and can be found both at the eastern and western ends
147 of the trench. At M2 there is a small vertical displacement attributed to E10. The other
148 cracks do not show visible displacements, which could be due to the erosive channelized
149 units (Cu1) lying atop of layer B2.

150 The channels unit (Cu1) can be divided into two main layers separated by an erosional

151 contact, which follows the base of the channel lenses. This contact marks the event
152 horizon for event E9.

153 The latter events broke and displaced the succession of sub-horizontal sandy layers. The
154 associated deformation is more concentrated in two main zones, one between M18 and
155 M16, the other at M9.

156 The event E8 is visible at M16, where the layers C and D are displaced downward
157 (~3cm). Cracks associated to E8 are also observed within layer E, but the top of layer E
158 is not deformed. Therefore, we consider that the event E8 occurred during the
159 deposition of layer E.

160 The next event, E7, corresponds to a set of small cracks at M17. These cracks reach the
161 top of the layer F, they are associated with a small vertical displacement. However, as
162 the layer F is made of fine laminated sand the presence of cracks is unambiguous.

163 Based only on trench observation, one cannot exclude that the cracks associated to E8
164 and E7 correspond only to accommodation faulting produced by more recent
165 earthquakes. Indeed some of them do not root deeply or seem to be shaped as a pull-
166 apart structure, which weakens the evidence for independent events.

167 The event E6 is defined by a set of faults reaching the layer H, which is a thin, brown
168 coarse layer. So it is difficult to see the end of the cracks. In addition, the base of this
169 layer is irregular so we cannot identify any displacement. The cracks, however, are
170 clearly visible in layers F and G, which are more laminated and made of finer materials.

171 Then event E5 is characterized by a limited number of cracks at M10-M9, they reach the
172 top of layer I. In this brown layer there is a small intermediate darker bed, which shows
173 a small vertical displacement.

174 The event E4 is not well marked in the trench. A series of cracks goes through the fine
175 yellow sandy layer (layer J), but it is unclear if they stop at the top of layer J or if they
176 also affect the layer above. Indeed, on the top of layer J sits a thin discontinuous layer of
177 gravels where the deformation might be difficult to recognize.

178 The next event, E3, caused a major deformation in this area. There are series of cracks at
179 M17 and at M9, which stop at the top of a layer K, a fine pinkish sandy layer, with almost
180 no clasts. The deformation due to this event is clearly identified in the eastern part. At
181 M9 the layers I, J, and K are clearly displaced downward (~25cm). The amount of
182 displacement is actually larger than the displacement affecting layers directly above
183 these units, attesting for a separate event. Its continuation in the western part of the
184 trench is less clear because of the uncertainty on the identification of layer K at this
185 place. But if we assume that layer K continues westward across the trench, although
186 facies changes significantly, all cracks between M3-M7 reaching the base of the
187 channelized unit (Cu3) would also match with the event horizon of E3.

188 The next event is associated to another series of cracks stopping at the base of layer L.

189 This series is located at M8 and M4 in an erosive channels unit deposited on top of the
190 scarp of event E3, so the associated event, E3Supp postdates E3.

191 The event E2 is associated with a series of cracks located in the main zone of
192 deformation (M18-M16). Its event horizon corresponds to the top of a sandy layer
193 containing cobbles and some small gravel lenses (layer L). Between M17 and M16 this
194 event produced an important vertical displacement (6-9cm), which is clearly visible in
195 the layer I, K, and L.

196 The last event is marked by two sets of fractures located in the two mains zones of
197 deformation (M18 and M9), these cracks reach the top of layer M, a light pink laminated
198 sandy unit. Only minor deformation is associated to these cracks visible in the trench.

199 There is also a small group of cracks affecting only the unit A. As unit A eroded on the
200 top, there is no offset associated to these cracks, but they are clearly identifiable through
201 a succession of oriented gravels and pebbles.

202

203 3. Timing of events and Identification of historical earthquakes

204

205 Time constraints were derived from accelerator mass spectrometry (AMS) radiocarbon
206 dating of detrital charcoals. The trench exposure presents a relatively rich and well-
207 distributed amount of datable material. 32 charcoals coming from the two walls of the
208 trench were dated (Tablesup 1, Fig. S4), we mainly used material from the southern
209 wall, and few charcoals were collected on the other wall (charcoals 2, 9, 11, 17, 100, 119,
210 123) when there was no datable material on a layer in the studied wall. Only 4 samples
211 (37,60, 71,79) had to be rejected, because their ages were significantly older than the
212 other ages, relatively to their stratigraphic position. We interpreted them as likely
213 reworked samples.

214 The time record is relatively complete and regular (Fig. S4) at least for the upper units,
215 *i.e.* for the last 3ky. For the lower units in the trench, several erosive contacts have been
216 identified. General continuity in our age distribution (Fig. S4), however, indicates that if
217 we have hiatus in our trench, they have to represent only short periods of time,
218 minimizing our chances to miss a major earthquake in our sedimentary record. The unit
219 A is the oldest unit and dates back to 9 ky B.P., the layer at the base of the trench (B2) is
220 dated at 8 ky BP. The chronological sequence is refined by combining a-priori
221 information from stratigraphy relationship and ¹⁴C ages in the Bayesian analysis
222 approach of Oxcal⁶. According to the locations of the samples, phases have been defined
223 to group samples that belong to the same unit and could not be clearly ordered based on
224 stratigraphic position (Fig. S4).

225

226 The Taybeh trench exhibits evidence for at least 11 paleoearthquakes, and one more
227 uncertain event. These earthquakes occurred during a period covering 8 ky (Fig. S5). We
228 benefit from solid time constraints for the last 3 ky, which is also the period when
229 historical and archaeological data are more numerous and accurate. However, no
230 datable material could be found between the event horizons of E4 and E5, making the
231 dating of this pair of events difficult because we cannot discriminate correctly these two
232 events. The cracks affecting only the push-up structure are not dated, as the age of this
233 unit is around 7000BC and this is the oldest unit of the trench. We only know that these
234 cracks developed before the deposit of layers G and I, which are erosive on unit A.

235

236 In the following, each event in the Taybeh trench is identified by combining dating
237 obtained using Oxcal and historical descriptions, which cover a wide region. All locations
238 mentioned in this text are indicated on Figure S6. In the area, the historical reports are
239 numerous and continuous in space and time. They give indications about the size of the
240 earthquakes and thus contribute to constrain their lateral extent. For this area the
241 seismites recorded in the Dead Sea are another source of information on earthquakes.
242 Seismites are indicators of earthquakes occurrence in the area. They are intraclast
243 breccia, which result from turbulences in the soft sediment⁷ created by strong shaking.
244 They record earthquakes from the whole Levantine area and not only earthquakes
245 rupturing faults located in the proper Dead Sea basin. They are good markers to
246 evaluate basin effects and recurrence patterns. We used seismites to support the
247 existence of an earthquake and to constrain the epicentral distance of earthquakes from
248 the Dead Sea⁷.

249

250 The three older events are poorly constrained in age as datable material has been very
251 limited. The conglomerates at the base of the trench includes only one sample (17) for
252 which dating gives a wide age range. Likewise the events E10 and E9 are not well
253 constrained as their event horizons are surrounded by thick layers containing only one
254 or two samples, which give us only an approximation of the ages of the layers. Hence, the
255 time intervals given by Oxcal are too wide to estimate properly an age. The age for E11,
256 E10 and E9 are respectively between 6.1 ky BC and 5.4 ky BC, between 4.6 ky BC and 4
257 ky BC, and between 2.4 ky BC and 956 BC (Fig. S5). The poor dating associated with the
258 lack of historical data for this time makes the matching of these events with specific
259 historical earthquake impossible. We can only notice the vague mention of two events in
260 2100 BC and 1050/1070 BC in the area, more or less confirmed by archaeological
261 remains^{8,9} and the existence of seismites in the Dead Sea, which correlate with these two
262 events^{7,10}.

263 The events E8, E7 and E6 are better constrained. Even if historical data about
264 earthquakes during the corresponding periods are scarce, we can still propose a specific
265 matching historical earthquake for each of these events:

266 The event E8 is dated between 885 BC and 514 BC (Fig. S5). This time interval is wide
267 but covers only few documented events, although only one is described in details. In 759
268 BC an earthquake produced great destructions and many casualties in Judea, Samaria
269 and Galilee¹¹. Zachariah gave around 520 BC (i.e., ~240 years later) a detailed
270 description of the event, where he described a large landslide developing on the Mount
271 of Olives, southeast of Jerusalem, without a clear origin. He suggests that it could be due
272 to an earthquake⁹. All the descriptions of this event concern the north of the Dead Sea.
273 Ferry et al.¹² also reported an event in a trench in the Jordan Valley that they associate to
274 the 759 BC event. Finally, in their study of cores from the Dead Sea Kagan et al.⁷
275 identified two events on the mid 8th century BC. Historical information about an event in
276 this period refers mainly to the Jordan valley event, but the event E8 could be the second
277 event observed by Kagan et al.⁷, even if it remains uncertain in view of the scarce data.

278 The event E7 is modeled between 520 BC and 280 BC (Fig S5), as for E8 the time interval
279 is wide and very little information about events in this period is available. We could
280 correlate this event with a down-faulting event along the northwestern tip of the Gulf of
281 Aqaba, which is recorded by a buried coral-reef platform^{13,14}. This event has been dated
282 using ¹⁴C and U-series on coral and yields ages of ~2.4 ka BP, which is in agreement
283 with the seismic period of E7. Moreover in the Qatar trench¹⁵ an earthquake is identified
284 for a period partly similar between 313 BC and 213 BC. It seems that the event E7
285 ruptured the central and southern part of the Wadi Araba. The northern limit remains
286 uncertain, but as there is no indication of an event in the 4th century BC in the cores of
287 the Dead Sea basin^{7,10} it seems that this event stopped before the Dead Sea basin,
288 probably in the area of Taybeh.

289 The time interval associated to the event E6 is narrow, between 160 BC and 117 BC (Fig.
290 S5). This period is compatible with a seismic layer dated about mid-2nd century BC that
291 was consistently documented all around the Dead Sea basin, and was associated to a
292 large magnitude event, which would have affected the northern part of the Dead Sea
293 fault^{7,10}. We cannot really conclude about this event, as there is absolutely no mention of
294 an earthquake in the southern part of the area. This event might actually be a small
295 event triggered by a larger one, which occurred north of the Dead Sea, or could have
296 ruptured the northern part of the Wadi Araba and be amalgamated with another event.
297 In this cases the fact that the Wadi Araba is relatively sparsely populated contrary to the
298 Jordan Valley would explain why there is no historical report about this small event in
299 this region.

300 Events E5 and E4 are recorded in two successive layers in the trench, which are not

301 dated, thus they are associated to the same period. E4 and E5 are modeled respectively
302 between 80 BC and 141 AD and between 14 BC and 205 AD (Fig. S5). Around the
303 beginning of this era two events are described in the region of the Dead Sea, Judea and
304 Wadi Araba, the 31 BC event and the 114 AD event. The 31 BC event is only described in
305 Judea, during the Jewish War by the historian Flavius Josephus¹¹. However, the damage
306 seems greatly exaggerated, with a number of casualties larger than the actual population
307 of the region⁹. It has been proposed that the 31 BC event caused the abandonment of
308 Qunram, but without substantial proof¹¹. Ruptures associated to the 31 BC event were
309 not observed in the Jordan valley¹², and there is no archaeological evidence of this
310 earthquake in Judea. Apart from Josephus there is no descriptions of any damage in the
311 area, so this event may have occurred in the Wadi Araba, which would explain the weak
312 effect north to the Dead Sea. There is no event recorded for this period at Qatar¹⁵, which
313 suggests that it ruptured the northern part of the Wadi Araba and potentially the Lisan
314 peninsula segment too. This is consistent with the observations of Kagan et al.⁷, who
315 described an intrabasin seismite for this event. They locate the 31 BC event in a radius of
316 40 km around the Dead Sea.

317 The 110-114 AD event is attested only by archaeological data and is quite disputed.
318 Indeed damage is described in Petra, Masada, Avdat and several other sites along the
319 Petra-Gaza road^{9,16}. Nevertheless there is generally no direct evidence to suggest that
320 the damage is due to an earthquake and it has been proposed that they might result
321 from wars. There is one excavation site in Masada where the rooms seem 'filled with the
322 result of an earthquake'^{9,17}. The presence of a series of crack dated between 14 BC and
323 205 AD in the trench at Taybeh, i.e. at the same latitude as Petra but in the valley, could
324 argue in favor of an earthquake. The fact that there was only moderate damage could
325 indicate that this event was of limited magnitude. This event occurred around Taybeh,
326 potentially southward as there is no indication of an event at this time in the Dead Sea
327 cores. As this event is not observed in the Qatar trench¹⁵ it had to stop on the north of
328 the extensional jog of Yotvata. In the light of the archaeological data, we consider that E5
329 could correspond to the 31 BC event and occurred on the section between the Lisan
330 peninsula and Taybeh and E4 might be the 110-114 AD event and ruptured the central
331 Araba section. Nevertheless as there is little evidence for E5 in the trench, this event
332 remains uncertain and these cracks could also be associated to E4. Therefore, if one
333 considers that only E4 exists, archeological evidence suggests that E4 would be the 31
334 BC earthquake.

335 The event E3 is dated between 287 AD and 815 AD (Fig. S5). This time window is wide,
336 as the sandy layers I, J, K and L lacked datable organic matter. During this period two
337 events are described in the area south of the Dead Sea: the 363 AD event and the mid 8th
338 century AD crisis. We can also notice the occurrence of several earthquakes during the

339 7th century, but they are mostly described further north.
340 During the night of 363 May 18th two earthquakes occurred in the Levantine area. As
341 they are coeval it is difficult to separate the effects of the two shocks. Nevertheless it
342 seems that the second shock affected more the southern part of the region. A seiche was
343 reported on the southeastern coast of the Dead Sea, as well as much destruction in
344 southern Palestine localities and in the city of Petra⁹. Moreover, destructions of Roman
345 buildings are documented in Aila (Aqaba), which are well time-constrained through
346 dates of more than 100 coins found under collapsed walls, to be post 360 AD¹⁸. A
347 seismite of the Dead Sea could be unambiguously associated to this event⁷. As the 363
348 AD earthquake is visible in the Qatar trench, Klinger et al.¹⁵ proposed that this event
349 ruptured at least the southern section of the Wadi Araba, between Qatar and the Gulf of
350 Aqaba, the northern limit of this rupture remaining unknown.

351 During the 7th century AD three earthquakes were reported. One event occurred in 634
352 AD, which is described in Palestine, mainly in Jerusalem⁹, arguing for a location close to
353 the Dead Sea. The other two events occurred in 659/660: the first event occurred in
354 June and it affected the Palestine and many places in the Jordan Valley. The second, in
355 September, destroyed a great part of Jericho and several monasteries in the hills, East of
356 Jerusalem^{11,19}. Although these events are mostly described based on reports from
357 locations further north and around the Jordan Valley, the September 659 AD earthquake
358 was felt in a narrow area surrounding Jericho. Thus we proposed that this event
359 occurred along the Jericho segment. In fact, the June 659 AD event was located by
360 Langut et al.²⁰ in the northern Jordan valley, in the vicinity of Beit-shean, which would be
361 consistent with the 7th century event observed in the 3D trench by Wechsler et al.²¹.
362 Eventually, Haynes et al.²² have reported evidence of damaged water cistern in Tilah,
363 which are dated to the the 7th century, and might correspond the 634 AD event.

364 The mid 8th century AD event is confusedly described and it has been shown recently
365 that descriptions of different earthquakes were often aggregated into a single giant
366 earthquake; Ambraseys⁹ demonstrated that at least three large earthquakes struck the
367 region south of the Lebanese range between 746 AD and 757 AD. And although damage
368 is reported for many of the main cities of the region, it remains difficult to ascertain
369 epicentral locations for each of them based only on macroseismic data. One large event
370 in 749 AD took place in the Jordan valley and reached the north of the Sea of Galilee, as
371 shown by paleoseismological and archaeological studies^{12,23-25}. At Qatar Klinger et al.¹⁵
372 identified another event around the mid 8th century AD in the Wadi Araba. Moreover
373 there is also evidence for damage in the ancient cities of Aila¹⁸ and Petra²⁶. In the trench
374 at Tilah there is an event dated between the 7th and the 11th century AD²². The authors
375 propose that this event correspond to the 873 AD earthquake. Nevertheless this
376 earthquake is described only in Medina, which is more than 1000 km away. If the event

377 observed in Tilah is the 873 AD event, it has to be a very large event to be felt in Medina
378 and in this case it would have to be felt also in closer cities. In view of the absence of
379 historical reports about a 873 earthquake in Wadi Araba or Jordan Valley areas, we
380 assume that this event corresponds to the 8th century AD event, which is mentioned in
381 many places in the area, rather than the 873 AD event. Thus the mid 8th century AD
382 event might be recorded in Tilah, in this case there would be evidence of a 8th century
383 AD events all along the Wadi Araba, which argues for a correlation between E3 and one
384 earthquake occurring during this seismic crisis.

385 If we consider that E3 correspond to a 7th century AD, like the one observed in Tilah²², it
386 implies that E3 occurred on the section between Taybeh and Tilah in the 7th century and
387 two earthquakes occurred in the Wadi Araba during the 8th century AD, one between the
388 Gulf of Aqaba and Qatar¹⁵ and the other north of Tilah. While if we consider that E3
389 correspond to a 8th century AD event, it implies that the 7th century AD event observed
390 at Tilah correspond to an earthquake having ruptured the section from Tilah to the
391 Lisan Peninsula, and the 8th century AD crisis affected all the Wadi Araba.

392 We favor the second scenario and consider that the event E3 corresponds to a 8th
393 century AD event, as it implies a smaller number of events. Moreover it is more
394 consistent with the historical data, which point to a location further north for the 7th
395 century events^{9,11}. It signifies that the 363 AD event did not reach the site of Taybeh.

396 The event E3Supp is modeled between 819 AD and 1395 AD, a period during which
397 three earthquakes are described in the area: the 1068 AD event, the 1212 AD event and
398 the 1293 AD event.

399 In 1068 AD there were two events^{9,27}, the 1068 March 18 event, most probably located
400 south of the Dead Sea, and the 1068 May 29 event, located closer to northern Palestine,
401 which have been aggregated into a single giant earthquake in most of the early historical
402 accounts¹². During the March 1068 event almost the entire population of Aqaba was
403 killed and damage to mosques was reported as far as Medina and Cairo⁹. Furthermore
404 modifications of water springs are reported close to the city of Tabuk⁹. There is evidence
405 of surface ruptures associated to the 1068 event in the Avrona playa, close to
406 Eilat/Aqaba^{28,29}. This event is located by Klinger et al.¹⁵ between the site of Qatar, where
407 there are observations of the event, and the Gulf of Aqaba. A magnitude M_W 6.5 or
408 higher has been proposed using the length of the rupture⁵, which is in good agreement
409 with values proposed earlier, based on macroseismic reports and geomorphological
410 observations²⁸⁻³⁰. If we consider that the event E3Supp is the 1068 AD event, it means
411 that the 1068 AD event ruptured at least the section between the Gulf of Aqaba and
412 Taybeh, *i.e.* a section 110km long. This rupture length corresponds⁵ to a magnitude of
413 7.4 or higher, which is too large compared to the macroseismic reports. So we assume
414 that the event E3Supp visible at Taybeh is not the 1068 AD earthquake.

415 The 1212 AD event is mainly described in the south Levantine area. This earthquake
416 produced extensive damage in the city of Aila (Aqaba). It is also reported in Egypt, the
417 Monastery of St Catherine in Sinai was partly destroyed and the shock was strongly felt
418 in Cairo where several houses collapsed. Destructions were also reported in north of the
419 Wadi Araba, in Al-Karak and Al-Shobak on the Jordanian plateau⁹. Based on the damage
420 reports and geomorphological observations this event is considered as an important
421 event of about M_w 7.5^{7,10}. This event is clearly identified in the Dead Sea cores⁷ as well as
422 in the Qatar trench¹⁵. It has been proposed that this event occurred along the segment
423 between Qatar and the Gulf of Aqaba and potentially in the Gulf as well^{9,15}.

424 The 1293 AD event is mainly described in Karak, where it produced great damage in the
425 citadel. This event was also felt in Ramla and on the Palestinian coast from Gaza to
426 Qaqun^{27,31}. There are seismites in different places in the Dead Sea where this event is
427 clearly identified^{7,10}. This event is usually located on the eastern flank of the Dead Sea,
428 its southern limit is not defined accurately.

429 Regarding the ages the event E3Supp may correspond to the three earthquakes,
430 nevertheless the 1068 AD event is felt only on the southern part of the Wadi Araba and if
431 we consider a rupture from Taybeh to the Gulf of Aqaba it implies a larger earthquake
432 than it seems to be as regards to the historical descriptions. The 1212 AD and 1293 AD
433 events were both felt close to Taybeh, but following the damage reports the 1212 AD
434 event was bigger further south. Indeed most of the damage is recorded around the Gulf
435 of Aqaba, as St Catherine, which is much further south in the Sinai Mountains, and
436 present an important degree of destruction. This is more in agreement with a rupture in
437 the Gulf of Aqaba than in the Wadi Araba. Kagan et al.⁷ based on the seismite analysis
438 propose a distance of the epicentre from the Dead Sea for several earthquakes. In the
439 case of the 1212 AD event they propose a relatively large distance of about 250-300km,
440 which support the location of this event in the Gulf of Aqaba. That is why we propose
441 that the event E3Supp is the 1293 AD earthquake, which implies that this event
442 ruptured the section extending north of Taybeh, and 1212 AD ruptured from the Gulf of
443 Aqaba until Qatar.

444 The penultimate event, E2, is modeled between 1448 AD and 1714 AD (Fig S5). During
445 that interval, the only significant event reported in the area is a magnitude $M6-7$ event in
446 November 1458⁹. The main destructions related to this earthquake are in Jerusalem and
447 Al-Karak. There is no mention of this event neither in the Wadi Araba nor in Aqaba.
448 Nevertheless this event is recognized in most of the seismite sequences cored in the
449 Dead Sea^{7,10}, based on the seismite they proposed that the 1458 AD event occurred
450 relatively close to the Dead Sea, around 50 km away. It is observed in the trench at
451 Qatar¹⁵, it may also be one of the events recognized in the cores at Aqaba³². The rupture
452 did not reach Aqaba, otherwise the city would have been more affected. The northern

453 limit of this rupture remains uncertain as there is not any clear evidence of this event at
454 Tilah. Indeed in Tilah the most recent event is dated between 1155 AD and 1918 AD²², it
455 could correspond to the 1212 AD, 1293 AD, 1458 AD, 1546 AD and 1834 AD events. The
456 1212 AD event seems to have occurred further south than the other regarding the
457 damage reports. The 1546 AD event has been firstly described as a major earthquake in
458 many places in the north Dead Sea (Safed, Tiberias, Ramla, Jerusalem, Hebron, Karak,
459 and Nablus)⁸. These descriptions seem highly exaggerated it would rather be medium-
460 size event affecting mainly Jerusalem⁹. This is in agreement with a rupture located in the
461 area close to Jerusalem, probably along the northernmost west Dead Sea shore. The
462 1834 AD event caused damage in Jerusalem, Bethlehem, Madaba, Jaffa and Caesarea, the
463 associated area is large and make difficult to locate its epicentral region⁹, nevertheless
464 most of the sources are located North of the Dead Sea, so we consider that this event
465 occurred in the Jordan Valley. The descriptions of the 1293 AD and 1458 AD event are
466 located in the same area, so these descriptions are not discriminant to determine which
467 earthquake correspond to the last event visible at Tilah. Nevertheless we identified the
468 1293 AD event in the Taybeh trench, as it is not visible in Qatar that suggests that its
469 rupture extends north of Taybeh. Moreover it as been proposed that this event was
470 located close to Karak, the most affected city, in the northern Araba^{9,26}. So the last event
471 visible at Tilah might be the 1293 AD earthquake, it implies that the 1293 AD event
472 ruptured the section from Taybeh until the Lisan Peninsula, while the 1458 AD
473 earthquake stopped further south, probably at Taybeh. Based on the descriptions of the
474 destructions and the paleoseismological observations all-together we proposed that the
475 event E2 is the 1458 AD earthquake, which ruptured a section of the Wadi Araba fault
476 located between the site of Qatar and our site.

477 The last event is modeled between 1688 AD and 1799 AD (Fig. S5). Agnon²⁶ proposed
478 that the 1834 AD event occurred in the Wadi Araba and would correspond to the last
479 event observed at Tilah. Hence, regarding the dating the event E1 might be the 1834 AD
480 event. Nevertheless the descriptions of the 1834 AD event consistently locate this event
481 north of the Dead Sea and based on these reports we would favor a location in the
482 Jordan Valley area for this event.

483 For the 18th century there is no other major earthquake described in the south of the
484 Levant area. If there had been a large event during this period in the Wadi Araba, as it is
485 quite recent it should have been recorded in historical reports. Thus we consider that
486 the event E1 is a smaller event, likely a Mw~5 event, and since there is no large city in
487 this region, this event did not produce significant damage and was not described. Small
488 events can locally be recorded in trenches if the trench is close to the epicentre and if
489 they produced a surface rupture³³. In the catalogue we do not take this event into

490 account, as it is small and cannot be considered for the estimates of earthquake
491 recurrence.

492

493

494

495 4. Earthquake catalogue

496

497 In order to investigate the fault behavior and the regional seismic hazard along the
498 southern Dead Sea fault, we established an earthquake catalogue for the part of the Dead
499 Sea fault between the Gulf of Aqaba and the southern limit of Mount Lebanon. The
500 catalogue is built by combining data from the literature (historical data^{11,26,27,31,34-37} and
501 paleoseismological data^{12,15,22,25,29}) and paleoseismological results presented in this
502 work.

503 To build the catalogue we firstly determine a simplified geometry of the fault, which
504 describes the sections rupturing during an earthquake. The geometry we choose
505 contains 9 segments that are described hereafter: The Wadi Araba section is split in
506 three segments separated respectively by an extensional jog, the Yotvata playa, and a
507 compressional jog at Jabal al-Risha. Similarly, the Jordan Valley section is also split in
508 three segment: One segment parallels the western bank of the Dead Sea and ends just
509 north of Jericho. The central segment stretches between Jericho and the Beit-She'an
510 Valley, which is formed by the intersection of the Jordan valley fault (JVF) and the
511 Carmel-Gilboa Fault System (CGFS), which branches westward from the JVF. The exact
512 location where to end this segment in the Beit-She'an Valley is debatable, as the JVF and
513 CGFS interact over a several kilometers long zone. In any case this zone is limited to the
514 north by the northern margin of Beit-She'an Valley. The last segment extends from the
515 Beit-She'an Valley to the northeastern shore of the Sea of Galilee, where the Jordan fault
516 interacts with the Jordan Gorge section³⁸. North of the Sea of Galilee we defined two
517 segments, the Jordan Gorge segment and the Hula basin segment.

518

519 In a second step we matched past earthquakes with fault segments:

520 In the Wadi Araba for the southernmost segment, between Aqaba and Yotvata, we used
521 the catalogue proposed by Klinger et al.¹⁵. For the central and northern segments we
522 used mainly the data of the Taybeh trench, the detailed description of the location of
523 paleo-earthquakes on these segments is described above in this study.

524

525 Along the Jericho segment, we were able to relocate several events until the fifth
526 century: The most recent one is dated from July 1927. It was the first significant event
527 (Mw=6.3) in the region to be recorded worldwide by seismometers. These records

528 allowed assessing the epicentral location^{39,40}, which is on the western side of the Dead
529 Sea, close to Mitzpe Shalem³⁹. Another recent earthquake might have occurred on this
530 segment in 1834 AD. The 1834 AD event is mainly described north of the Dead Sea
531 especially in Jerusalem where several minarets and churches collapsed. Damage
532 associated to the 1834 AD earthquake was also reported in the cities of Bethlehem,
533 Madaba, Nablus, Caesarea and in the Dead Sea basin where asphalt floated⁹. Distribution
534 of seismite in the Dead Sea basin argues for an epicenter rather close to the basin⁷.
535 Hence, this event occurred in the Jordan Valley, very likely along the Jericho segment.
536 The historical descriptions of the 1546 AD event seem to indicate a similar intensity map
537 to the 1927 event, hence we locate the 1546 AD event on the same segment. The May
538 29th 1068 AD earthquake is known mostly to have destroyed al-Ramla. Only slight
539 damage is reported in the other places in the region. This event is mentioned briefly in
540 Jerusalem and Banias. Hence, the scarcity of historical descriptions and their
541 heterogeneities suggest a possible exaggeration of the damage. The area of distribution
542 of the damage linked to this event points to a location in the Jordan valley. Ferry et al.¹²
543 see only one event at this time in their trench, which is located in the central part of the
544 Jordan valley, and they suggest that it corresponds the 1033 AD event. Thus we assume
545 that the 1068 AD event occurred on the Jericho segment. However, owing to the lack of
546 historical data for this earthquake, its authenticity remains arguable^{26,31} and if it existed
547 magnitude might have been smaller than previously proposed. Thus for the scenario
548 considering the smallest extent for each earthquake (in light blue on fig 3, S7-S12) we
549 attributed a magnitude of 6.5 to this event. All the reported damage caused by the
550 September 660 AD event were located on the western flank of the Dead Sea, Jericho was
551 partly destroyed as well as several monasteries in this region, including St. John the
552 Baptist monastery. Thus we assume that the September 660 AD earthquake occurred
553 along the Jericho segment. This is also supported by the presence of seismites in at least
554 two cores drilled in the Dead Sea^{7,10}. Another event dating back to 419 AD has been
555 described in this area. However the available testimonies are less specific, several
556 Palestinian villages have been allegedly destroyed, indicating that this event occurred
557 along the Jordan valley. We favored the Jericho segment since Kagan et al.⁷ described it
558 as an intra basin seismite, implying that it took place close to the Dead Sea basin.

559

560 Along the central Jordan Valley segment, we used mainly the results of Ferry et al.¹² to
561 determine the chronology of earthquakes, except for the most recent events since the
562 upper part of their trenches are plowed soils. The 1033 AD event appears on all four
563 trenches both north and south of the segment¹². It was felt in Jerusalem – where
564 according to Ibn Al-Jawzi (A.D. 1113-1200) the walls were damaged while still in
565 construction - Ramallah, Jericho, Nablus and Tiberias and throughout Judea and Syria⁴¹.

566 Hence, we assigned this earthquake to the central part of the Jordan Valley fault,
567 although we could not rule out that it could also have ruptured the northern part of the
568 Jordan valley, in view of the macroseismic data. The second event recorded in Ferry's
569 trenches dates from 749 AD. Great destructions and many casualties have been reported
570 in Judea, Samaria and Galilee at this time¹¹. The mid 8th century is known in the Dead Sea
571 area as a period of intense seismic activity and historical descriptions tend to merge
572 multiple events together. Since this earthquake is also recognized in a trench north of
573 the Sea of Galilee²⁵, we consider that it ruptured all three segments (the central and
574 north Jordan valley segments and the Jordan Gorge segment).

575 Along the northern Jordan valley segment, the most recent event we identified is the 854
576 AD event. This earthquake caused several landslides around Tiberias, and many
577 casualties in the city due to collapses^{9,11}. Before this event, the 749 AD event ruptured all
578 the Jordan valley section. Another event described in this region is the 659/660 AD
579 earthquake, which was followed by a large series of aftershocks. This event was
580 reported in several places across Palestine^{11,20,31}. There is also some debatable evidence
581 of an earthquake proposed at Gerasa and Pella¹⁶. This report indicates a location of the
582 earthquake in the Jordan valley. We assume that it occurred on the northern segment
583 because there is no evidence of an event in the trenches on the central segment¹².
584 Furthermore Wechsler et al.²¹ describe an event around that time at a site on the
585 southern part of the Jordan Gorge in Beteiha. They propose that this event corresponds
586 to the 660 AD event, which corroborates a rupture in the northern area of the Jordan
587 valley. This earthquake would have ruptured the northern Jordan valley segment and
588 the Jordan Gorge segment.

589 The Jordan Valley section of the DST is interpreted to have ruptured during the March-
590 363 AD earthquake based on historical records⁹. The historical descriptions cover a
591 wide area, which extends from Banias in the north to Areopolis in the south. The
592 southern limit of the area where this earthquake was felt is not well constrained because
593 of the occurrence of another earthquake in the Wadi Araba the same year that lead to
594 some confusion in descriptions. The 363 AD event is not clearly identified in the
595 trenches on the central Jordan valley segment¹², nevertheless we can notice that there is
596 one event in these trenches dated before the 6th century AD, but the time constraint is
597 weak and it is not possible to conclude about the age of this event. As most of the site
598 that where damage during the 363 AD event are located west of the Jordan valley, it has
599 been proposed that this earthquake occurred on the Carmel fault²⁶. However such
600 asymmetry, which is observed for several events in the area, might also in part be
601 attributed to the difference of density of population between the Eastern and the
602 Western Levant. Moreover Wechsler et al.²¹ identified in the Beteiha trench
603 displacements associated to three events occurring on the 4th century AD. The authors

604 assume that one of these events could be the 363 AD event, so the 363 AD-earthquake
605 rupture reached as far north as the Beteiha valley. Based on this observation we
606 proposed that the 363 AD event ruptured the Jordan Valley fault. The southern limit
607 remains unclear, but in view of the historical report distribution this earthquake was
608 quite important and ruptured at least the northern segment of the Jordan Valley and
609 most probably the central segment too.

610 In addition to these events that are well described, there is also a series of events loosely
611 described during the 12 century, which are associated with the Jordan valley area. In
612 1113 AD the Christians in Jerusalem report two events occurring in the Kingdom of
613 Jerusalem (which lies from south to north between the northern Dead Sea basin to the
614 Sea of Galilee), likewise in 1114 AD an earthquake is described by authors living in
615 Jerusalem but as there is no indication of damage in Jerusalem, Ambraseys⁹ proposed
616 that it occurred around the Sea of Galilee. Finally, an event is described in Jerusalem in
617 1117 AD. All the reports of these events are vague and do not indicate significant
618 damage, so we assume that between 1113 AD and 1117 AD a series of smaller
619 earthquakes ($M_w \sim 6$) occurred all along the Jordan Valley.

620
621 The last main section, north to the Sea of Galilee is divided in two segments. The Jordan
622 Gorge Segment, which lies between the Sea of Galilee and the Hula basin. The other is
623 the Hula basin segment, which constitutes the western flank of this basin and stops
624 south of Mount Lebanon where the fault divides into two faults, the Roum fault to the
625 west and the Yamouneh fault to the east. These two segments are short ~ 20 km
626 compared to the others.

627 Along the Jordan Gorge segment, two 3D paleoseismological studies^{23,25} and one
628 archaeological sites^{42,43} provide indications about earthquake history. The 3D trenches
629 provide us with lateral displacement measurements across the fault. These
630 displacements correspond to co-seismic displacements associated with well-known
631 historical events, but a part of the displacement could also be due to aftershocks or local
632 events that were triggered by larger regional events. The 3D trenches show a dense
633 chronology of earthquakes²⁵. The most recent earthquake is the 1759 AD event, which
634 severely affected Lebanon. Two earthquakes actually struck the area in 1759 AD. The
635 larger shock on November 25th destroyed all the villages in the Beqaa valley. Baalbek
636 was ruined. Safed, Ras Baalbek, and Damascus were damaged, and the earthquake was
637 felt as far as Egypt and Anatolia, 1100 km away⁴⁴. A smaller earthquake occurred about
638 one month earlier, on October 30th 1759. This shock ruined Safed, Qunaitra, and many
639 villages nearby, and triggered a seismic seiche in the Sea of Galilee⁸. This later event is
640 also described at the Crusader castle of Vadum Jacob^{42,43} where it is associated to 0.5 m
641 of displacement, which is confirmed by the measurement in 3D trenches by Wechsler et

642 al.²¹. Studies on the Rachaya fault⁴⁵ and on the Serghaya fault^{46,47} showed that the two
643 1759 AD earthquakes occurred along these faults. So, the 1759 October earthquake
644 ruptured the Jordan Gorge segment and the Rachaya fault, while the November event
645 ruptured the Serghaya fault. The previous event recorded is the 1202 AD event, which
646 shook mainly Lebanon and western Syria. The cities of Baalbek, Nablus, Acre, Safed,
647 Tyre, Tripoli, among others, where severely damaged. Shaking was felt throughout the
648 Middle East⁴⁴. This event is also observed in the paleoseismological trench of
649 Yamouneh⁴⁸, and at the Crusader castle of Vadum Jacob^{42,43}. This earthquake occurred
650 on the Yamouneh fault, the Hula basin segment, and the Jordan Gorge segment. In the
651 Beteiha site, Wechsler et al.²¹ observe 2.1 m of displacement associated to this event,
652 such as Ellenblum et al.⁴³ in Vadum Jacob. The 3D trench also exposes evidence for a 1.2
653 m displacement linked to the 749 AD earthquake²¹. This event is known to have
654 ruptured the Jordan valley section¹², and the presence of surface rupture associated to
655 this earthquake north of the Sea of Galilee implies that this event extended further north
656 than expected and the Jordan Gorge segment correspond to the northern limit of the
657 rupture. We consider here that the 749 ad earthquake reached the Beteiha valley but do
658 not ruptured all the Jordan Gorge segment as there is less mention of this event in
659 Lebanon. There is possibly an event during the 7th century AD that is recorded in the
660 trench at the Beteiha site in the Jordan Gorge. The occurrence of this event remains
661 unclear, as the associated displacement is small (almost non-existing). We assume that
662 this 7th century event corresponds to the June 659 AD earthquake, which occurred on
663 the Jordan valley section and extended a little north. Another event with a displacement
664 about 1.2 m is recorded in the 3D trench, the displaced deposits give an age for the
665 seismic event between 505 and 593 AD. During that period several earthquakes caused
666 damage in the region, but mostly on the coastal area. It is the case for the 502 AD and
667 551 AD earthquakes. Paleoseismic studies point to the offshore Lebanese thrust system
668 as the most likely source of the 551 AD earthquake⁴⁹. So we could tentatively associate
669 the displacement in the trench with the 502 AD event, even if an offshore source appears
670 more consistent, as this event mainly destroyed Acre, Sidon, Tyr, and to a lesser degree
671 Beirut. In that case, the 502 AD earthquake would have ruptured the Jordan Gorge
672 segment, the Hula basin segment, and the Roum fault. Moreover, as the 4th-8th century
673 AD period is well documented historically, chances that an additional historical event,
674 with more than 1 m of slip, went unnoticed is unlikely^{35,37}. In the 3D trench at the
675 Beteiha valley the oldest displaced channel records evidence for six additional
676 earthquakes. Two of them affected the upper units with additional cumulative slip of 1.8
677 to 3.6 m. Both are likely moderate in size, each with 0.9-1.8 m of horizontal slip. Three of
678 the six earthquakes were dated in the 4th century AD, including the two events that
679 affected the upper units. The authors proposed that it is the 303 AD, 348 AD and 363 AD

680 events. The 303 AD event caused damage mostly on the southern Lebanese coast (Sidon
681 and Tyr). The 343 AD event is described in Beirut, where a large part of the city was
682 ruined. The 343 AD event could also be associated to the penultimate event visible in the
683 Yamouneh trench, which is dated between 30 BC and 469 AD⁴⁸, which could explain why
684 most of the reports are further north. However, in this case the rupture length of this
685 event is quite important as it extends from the Jordan Gorge to the Yamouneh fault, just
686 as the 1202 AD earthquake, which is in disagreement with the limited available
687 historical reports. The 363 AD event is known to have ruptured the Jordan Valley
688 section, as most of the historical reports for this event are in Palestine and around the
689 Jordan Valley. The presence of a rupture in the Beteiha trench implies that the rupture
690 extended also a little north of the Sea of Galilee. The ages of the three other events are
691 not well constrained, two of them are dated from the 2nd century. Associated
692 displacements are not clear and in any case quite small. One of them could be associated
693 with the 130 AD earthquake, which caused damage at Caesarea, but the reports are very
694 unclear even about the location of the city. Finally, the oldest event visible in the trench
695 is associated to a large displacement and dated between 392BC and 91 AD. Ellenblum et
696 al. 2015⁵⁰ find evidence of a coseismic offset under the castle of Vadum Jacob, reaching
697 ~2.5m dated to circa 142 BC. So we propose that the oldest event at Beteiha could be the
698 140 BC event, which was described along the Lebanon coast^{8,9}. This event was
699 associated to a large magnitude⁸, which is in accord with the measured displacement.
700 Ellenblum et al. 2015⁵⁰ also point to a post Hellenistic event, with an abandonment of
701 the site around the mid-first century BC, for which we do not propose a specific
702 earthquake correlation.

703 The Hula basin segment is small and located between the intersection of the Roum and
704 Yamouneh faults in the north and the intersection of the Rachaya and Jordan Gorge
705 faults in the south. This segment behaves like an inter-segment due to its particular
706 location, *i.e.* this segment breaks only with others surrounding segments of the fault. As
707 a result, in order to identify the events that occurred on the Hula basin segment we
708 firstly investigated earthquakes occurring on the Roum and Yamouneh faults. On the
709 Roum fault only one event is well identified during the historical times. Nemer et al.⁵¹
710 dug a trench on the Roum fault and identified an event that occurred after the 3rd
711 century AD, based on historical reports it could be the 551 AD or 1837 AD event. As the
712 551 AD earthquake is well located offshore of Lebanon⁴⁹, they assume that it is the 1837
713 AD earthquake. Destructions or heavy damage caused by this earthquake extended
714 along a relatively narrow zone from the coastal area of Sidon to the Sea of Galilee. Sidon
715 was the most damaged location. Damage was also reported in Beirut, along the Bekaa
716 valley, at Banias, the area of the Sea of Galilee is also affected. South to the Sea of Galilee
717 the damage is weaker. We assume that the 1837 AD earthquake ruptured the Roum fault

718 and the Hula basin segment. The Hula basin segment also ruptured during the 1202 AD
719 earthquake, for which there are surface ruptures attested on the Yamouneh fault and on
720 the Jordan Gorge fault. The 348 AD event, which is described in the Beteiha trench,
721 seems to have ruptured the section coming from the Yamouneh fault, so it must have
722 ruptured also the Hula basin segment. The last event we located along this segment is
723 more uncertain, namely the 198 BC event. At this time there was a series of shocks felt in
724 the region of Sidon, and almost two thirds of the city collapsed. It could correspond to
725 the second event described in the trench on the Roum fault⁵¹, although as the time
726 interval associated to this event is wide, reaching conclusion remains hazardous. In this
727 case the 198 BC might have ruptured the Roum fault and the Hula basin segment.

728
729
730
731

732 5. Alternative rupture scenarios

733

734 For several events described previously we have seen that uncertainties remain about
735 their extensions and limits, or even their locations. In the precedent sections we have
736 presented the historical and paleoseismological data about past earthquakes available in
737 the area, and then our favorite scenario. Here we will focus on possible alternatives for
738 this scenario and evaluate the impact on our output model.

739 Most alternatives deal with the Wadi Araba, and the identification of historical events at
740 Taybeh and Tilah. We present only one change concerning solely the area north of the
741 Dead Sea.

742

743 Alternative 1: the northern limit of the 363 AD and 749 AD ruptures along the Jordan
744 Gorge segment is located further north

745 Our favorite scenario considers that the 363 AD and 749 AD earthquakes, observed in
746 the Jordan Valley trenches and widely reported in this area, ruptured the north Jordan
747 Valley section up to Beteiha, but not the entire Jordan Gorge segment, as they are
748 described in the 3D trench by Wechsler et al.²¹ but not in the Vadum Jacob site⁵⁰. In
749 figure S7 the slip deficit is calculated considering that these events ruptured also the
750 Jordan Gorge section. This change implies a slightly smaller calculated slip deficit in the
751 Jordan Valley although it does not impact our conclusion. Indeed, for the 749 AD
752 earthquake we always used the co-seismic displacement measured in trench²¹ to assess
753 the lower slip-deficit value.

754

755 Alternative 2: effect of the location of the northern limit of the 363 AD rupture

756 At Taybeh we propose that the event E3 correspond to a 8th century event, which
757 implies that the 363 AD event does not reach Taybeh. We previously limited the rupture
758 of the 363 AD event to the southern Wadi Araba segment. Nevertheless as strike-slip
759 ruptures do not always stop at fault discontinuities⁵², we can wonder if this earthquake
760 extends further north. In figure S7 we consider that the 363 AD event ruptured the
761 southern and central segments of the Wadi Araba, and stopped at the southern limit of
762 the Risha compressional jog. This modification reduces the slip deficit the central Araba
763 segment to 0.7 m and leads to relatively small values of slip deficit in the Wadi Araba.

764

765 Alternative 3: the event E3 is associated to a 7th century AD earthquake

766 Another debatable point is the identification of E3 as a 8th century AD event rather than
767 a 7th century AD event as in Tilah. Indeed in Tilah Haynes et al.²² described two events
768 during this period, one in the 7th century AD and another between the 7th and the 11th
769 century AD, whereas there is only one event recorded at Taybeh for this period. We
770 firstly favor a scenario with a large 8th century AD event in the whole Wadi Araba and a
771 small 7th century AD event in the north. In figure S8 we present a scenario with a 7th
772 century event between Taybeh and Tilah and two 8th century AD events. This scenario
773 leads to very large slip deficits in the Wadi Araba, up to 7.2 m. Accommodating such
774 large slip deficit in one earthquake implies very large magnitude ($M > 7.5$) earthquake,
775 which have not been documented along the DSF so far.

776

777 Alternative 4: combination of alternatives 2 and 3

778 The previous two alternative scenarios have opposite effects. Thus we tested both
779 changes together (figure S9). We observe that the lengthening of the 363 AD event is not
780 enough to compensate the shortening of the 8th century AD event. That support again
781 the fact that very large earthquakes occur occasionally.

782

783 Alternative 5: effect of the location of the northern limit of the 1293 AD earthquake

784 Another debatable point is the limit of the 1293 AD event. We previously considered
785 that the 1293 AD event was visible at Taybeh and Tilah, thus it would have ruptured the
786 section from Taybeh to the Lisan Peninsula. Nevertheless, the dating of the events at
787 Tilah allows for another interpretation, with a 9th century AD event. We present in figure
788 S10 an alternative of our scenario with a 9th century AD event located on the Lisan
789 Peninsula segment and the 1293 AD event, which is recorded at Taybeh, to rupture the
790 section between Taybeh and Tilah. This scenario increases significantly the slip deficit
791 on the concerned segments. This supports the fact that the 1293 AD earthquake
792 ruptures both sections.

793 It is note worthy that if we consider that the 1293 AD earthquake ruptured the area
794 from Taybeh to the Lisan Peninsula and that there is an additional event on the Lisan
795 Peninsula during the 9th century AD, the slip deficit would decrease slightly. For the
796 Lisan Peninsula section the slip deficit is then of 0.9 m (this scenario is not represented).
797

798 Alternative 6: the last event observed at Taybeh is correlated to the 1834 AD event:
799 The last event observed in Taybeh is dated during the 18th century AD, as no major
800 earthquake is described in the southern Dead Sea area we proposed that it could be a
801 minor event, like a Mw 5-6 earthquake, locally recorded. But Agnon 2014²⁶ proposed
802 that the 1834 AD event correspond to the last event recorded in Tilah. In that case the
803 last event at Taybeh might also correspond to the 1834 AD event. In figure S11 we
804 present the corresponding slip deficit. The deficit of the northern Wadi Araba segment is
805 reduced to 0.7m, which appears sensible. Nevertheless it increased noticeably the deficit
806 in the Jordan Valley, where we have previously located the 1834 AD event. This scenario
807 tends to increase the heterogeneity in the slip deficit along the fault. Moreover this
808 location for the 1834 AD event is not fully consistent with the historical reports.
809

810 Alternative 7: impact of the occurrence of the 114 AD event:
811 Finally as explained previously the event E5 remains ambiguous because of the few
812 cracks visible in the trench and the controversial historical descriptions. Thus we
813 propose an alternative scenario, which does not take into account the 114 AD event,
814 which is presented in figure S12. In this case the balance is realized on more than 2000
815 years, and the accumulated slip deficit increases noticeably, which might be another
816 evidence of the occurrence of this earthquake. Nevertheless if we consider that the 363
817 AD event ruptured also the central part of the Wadi Araba, which is a plausible
818 alternative as explained before, the effect of the 114 AD event is not visible anymore in
819 our balance, as this one is realized for the period since the 4th century AD crisis.
820

821 These alternative models show that scenarios, which do not include large events, are
822 associated to very large deficit, until 7m (Fig S8). These values appear quite unrealistic,
823 which suggests that large earthquake occur episodically in the area.
824

825 6. Probability computation

826

827 To compute the probability of occurrence of an earthquake we followed the “empirical”
828 model of Savage⁵³. Savage proposed that the conditional probability of a future event
829 might be estimated from the observed recurrence intervals. His method was later
830 extended to include dating uncertainties of paleoseismic series⁵⁴. The catalogue

831 presents a number n of intervals for each segment. We count the number m of n
 832 intervals that are shorter than the period since the last event $(T, T+\Delta T)$. With success
 833 defined as an event falling in the interval $(T, T+\Delta T)$, and failure otherwise, the
 834 distribution governing the probability p of a future event in $(T, T+\Delta T)$ follows a beta
 835 distribution⁵⁴:

836

$$837 \quad P(p|m,n) = \frac{(n+1)!}{m!(n-m)!} p^m (1-p)^{n-m}$$

838

839 For this distribution the mean and variance are respectively, $\bar{p} = (m+n)/(n+1)$ and
 840 $\sigma^2 = \bar{p}(1-\bar{p})/(n-3)$. We define a confidence interval (C.I.) and determine p_{lo} and p_{hi} , as
 841 the 5% and 95% boundaries of P :

842

$$843 \quad \int_{-\infty}^{p_{lo}} P(p|m,n) dp = 0.05 \quad \text{and} \quad \int_{-\infty}^{p_{hi}} P(p|m,n) dp = 0.95$$

844

845 And C.I. corresponds to the integral of $P(p|m,n)$ between p_{lo} and p_{hi} . We discuss only
 846 values of the C.I. that we consider as more representative to assess the seismic hazard.

847 Usually the estimated probability improves with a longer record, but the large
 848 uncertainties in the empirical distribution of conditional probabilities show that even
 849 the present long paleoseismic series do not necessarily constrain uncertainties better
 850 when relatively few interval lengths are longer than the open interval since the last
 851 event.

852

853

854 7. References

855

- 856 1. Migowski, C., Stein, M., Prasad, S., Negendank, J. F. W. & Agnon, A. Holocene
 857 Climate Variability and Cultural Evolution in the Near East from the Dead Sea
 858 Sedimentary Record. *Quaternary Research* **66**, 421–431 (2006).
- 859 2. McCalpin, J. P. *Paleoseismology*. **95**, (Academic press, 2009).
- 860 3. Le Béon, M. *et al.* Slip rate and locking depth from GPS profiles across the southern
 861 Dead Sea Transform. *J. Geophys. Res.* **113**, 281–19 (2008).
- 862 4. Masson, F., Hamiel, Y., Agnon, A., Klinger, Y. & Deprez, A. Variable behavior of the
 863 Dead Sea Fault along the southern Arava segment from GPS measurements.
 864 *comptes rendus geoscience* **347**, 1–9 (2015).
- 865 5. Wells, D. L. & Coppersmith, K. J. New empirical relationships among magnitude,
 866 rupture length, rupture width, rupture area, and surface displacement. *Bulletin of*
 867 *the Seismological Society of America* **84**, 974–1002 (1994).
- 868 6. Ramsey, C. B. Bayesian Analysis of Radiocarbon Dates. *Radiocarbon* **51**, 337–360
 869 (2009).
- 870 7. Kagan, E., Stein, M., Agnon, A. & Neumann, F. Intrabasin paleoearthquake and
 871 quiescence correlation of the late Holocene Dead Sea. *J. Geophys. Res.* **116**, 195–27
 872 (2011).

- 873 8. Ben-Menahem, A. Four thousand years of seismicity along the Dead Sea Rift.
874 *Journal of Geophysical Research: Solid Earth* **96**, 20195–20216 (1991).
- 875 9. Ambrasseys, N. *Earthquakes in the eastern Mediterranean and the Middle East: a*
876 *multidisciplinary study of 2000 years of seismicity*. (2009).
- 877 10. Migowski, C., Agnon, A., Bookman, R., Negendank, J. F. W. & Stein, M. Recurrence
878 pattern of Holocene earthquakes along the Dead Sea transform revealed by varve-
879 counting and radiocarbon dating of lacustrine sediments. *Earth and Planetary*
880 *Science Letters* **222**, 301–314 (2004).
- 881 11. Guidoboni, E., Comastri, A. & Traina, G. *Catalogue of ancient earthquakes in the*
882 *Mediterranean area up to the 10th century*. (Istituto Nazionale di Geofisica, 1994).
- 883 12. Ferry, M., Meghraoui, M., Karaki, N. A., Al-Taj, M. & Khalil, L. Episodic behavior of
884 the Jordan Valley section of the Dead Sea fault inferred from a 14-ka-long
885 integrated catalog of large earthquakes. *Bulletin of the Seismological Society of*
886 *America* **101**, 39–67 (2011).
- 887 13. Shaked, Y. *et al.* Large earthquakes kill coral reefs at the north-west Gulf of Aqaba.
888 *Terra Nova* **16**, 133–138 (2004).
- 889 14. Shaked, Y., Lazar, B., Marco, S., Stein, M. & Agnon, A. Late Holocene events that
890 shaped the shoreline at the northern Gulf of Aqaba recorded by a buried fossil
891 reef. *Israel Journal of Earth Sciences* **58**, 355–368 (2011).
- 892 15. Klinger, Y., Le Beon, M. & Al-Qaryouti, M. 5000 yr of paleoseismicity along the
893 southern Dead Sea fault. *Geophys. J. Int.* **202**, 313–327 (2015).
- 894 16. Russell, K. W. The earthquake chronology of Palestine and northwest Arabia from
895 the 2nd through the mid-8th century AD. *bulletin of the American schools of*
896 *oriental research* **260**, 37–59 (1985).
- 897 17. Yadin, Y. The Excavation of Masada—1963/64: Preliminary Report. *Israel*
898 *Exploration Journal* **15**, 1–120 (1965).
- 899 18. Thomas, R., Niemi, T. M. & Parker, S. T. Structural damage from earthquakes in the
900 second: ninth centuries at the archaeological site of Aila in Aqaba, Jordan. *bulletin*
901 *of the American schools of oriental research* **346**, 59–77 (2007).
- 902 19. Amiran, D. H., Arieah, E. & Turcotte, T. Earthquakes in Israel and adjacent areas:
903 Macroseismic observations since 100 BCE. *Israel Exploration Journal* 260–305
904 (1994).
- 905 20. Langgut, D., Yannai, E., Taxel, I., Agnon, A. & Marco, S. Resolving a historical
906 earthquake date at Tel Yavneh (central Israel) using pollen seasonality. *Palynology*
907 **40**, 145–159 (2015).
- 908 21. Wechsler, N., Rockwell, T. K. & Klinger, Y. Variable slip-rate and slip-per-event on a
909 plate boundary fault: The Dead Sea fault in northern Israel. *Tectonophysics* **722**,
910 210–226 (2018).
- 911 22. Haynes, J. M., Niemi, T. M. & Atallah, M. Evidence for ground-rupturing
912 earthquakes on the Northern Wadi Araba fault at the archaeological site of Qasr
913 Tilah, Dead Sea Transform fault system, Jordan. *J Seismol* **10**, 415–430 (2006).
- 914 23. Marco, S., Rockwell, T., Heimann, A., Frieslander, U. & Agnon, A. Late Holocene
915 activity of the Dead Sea Transform revealed in 3D palaeoseismic trenches on the
916 Jordan Gorge segment. *Earth and Planetary Science Letters* **234**, 189–205 (2005).
- 917 24. Marco, S. Recognition of earthquake-related damage in archaeological sites:
918 Examples from the Dead Sea fault zone. *Tectonophysics* **453**, 148–156 (2008).
- 919 25. Wechsler, N. *et al.* A Paleoseismic Record of Earthquakes for the Dead Sea
920 Transform Fault between the First and Seventh Centuries C.E.: Nonperiodic
921 Behavior of a Plate Boundary Fault. *Bulletin of the Seismological Society of America*

- 922 **104**, 1329–1347 (2014).
- 923 26. Agnon, A. in *Dead Sea Transform Fault System: Reviews* (eds. Garfunkel, Z., Ben
924 Avraham, Z. & Kagan, E.) **6**, 207–261 (Springer Netherlands, 2014).
- 925 27. Guidoboni, E. & Comastri, A. *Catalogue of Earthquakes and Tsunamis in the*
926 *Mediterranean Area from the 11th to the 15th Century*. (Istituto nazionale di
927 geofisica e vulcanologia, 2005).
- 928 28. Amit, R., Zilberman, E. & Enzel, Y. Paleoseismic evidence for time dependency of
929 seismic response on a fault system in the southern Arava Valley, Dead Sea rift,
930 Israel. *Geological Society of America Bulletin* **114**, 192–206 (2002).
- 931 29. Zilberman, E., Amit, R., Porat, N., Enzel, Y. & Avner, U. Surface ruptures induced by
932 the devastating 1068 AD earthquake in the southern Arava valley, Dead Sea Rift,
933 Israel. *Tectonophysics* **408**, 79–99 (2005).
- 934 30. Klinger, Y., Avouac, J. P., Dorbath, L., Abou Karaki, N. & Tisnerat, N. Seismic
935 behaviour of the Dead Sea fault along Araba valley, Jordan. *Geophys. J. Int.* **142**,
936 769–782 (2000).
- 937 31. Ambrasseys, N. *Earthquakes in the eastern Mediterranean and the Middle East: a*
938 *multidisciplinary study of 2000 years of seismicity*. (2009).
- 939 32. Kanari, M., Ben-Avraham, Z., Tibor, G. & Bookman, R. On-land & Offshore Evidence
940 for Holocene Earthquakes in the Northern Gulf of Aqaba-Elat, Israel/Jordan. in
941 (2015).
- 942 33. Zeng, J. L., Shao, Y., Klinger, Y. & Xie, K. Variability in magnitude of
943 paleoearthquakes revealed by trenching and historical records, along the Haiyuan
944 fault, China. *Journal of Geophysical Research: Solid Earth* **120**, (2015).
- 945 34. Karcz, I. Implications of some early Jewish sources for estimates of earthquake
946 hazard in the Holy Land. *Annals of Geophysics* **47**, 759–792 (2004).
- 947 35. Sbeinati, M. R., Darawcheh, R. & Mouty, M. The historical earthquakes of Syria: an
948 analysis of large and moderate earthquakes from 1365 BC to 1900 AD. *Annals of*
949 *Geophysics* **48**, (2005).
- 950 36. Marco, S. & Klinger, Y. in *Dead Sea Transform Fault System: Reviews* (eds.
951 Garfunkel, Z., Ben Avraham, Z. & Kagan, E.) **6**, 183–205 (Springer Netherlands,
952 2014).
- 953 37. Zohar, M., Salamon, A. & Rubin, R. Reappraised list of historical earthquakes that
954 affected Israel and its close surroundings. *J Seismol* **20**, 971–985 (2016).
- 955 38. Ben Avraham, Z., Brink, ten, U., Bell, R. & Reznikov, M. Gravity field over the Sea of
956 Galilee: Evidence for a composite basin along a transform fault. *Journal of*
957 *Geophysical Research: Solid Earth* **101**, 533–544 (1996).
- 958 39. Avni, R., Bowman, D., Shapira, A. & Nur, A. Erroneous interpretation of historical
959 documents related to the epicenter of the 1927 Jericho earthquake in the Holy
960 Land. *J Seismol* **6**, 469–476 (2002).
- 961 40. Zohar, M. & Marco, S. Re-estimating the epicenter of the 1927 Jericho earthquake
962 using spatial distribution of intensity data. *Journal of Applied Geophysics* **82**, 19–29
963 (2012).
- 964 41. Abou Karaki, N. Synthèse et carte sismotectonique des pays de la bordure
965 orientale de la Méditerranée: sismicité du système de failles du Jourdain-Mer
966 Morte. (Strasbourg 1, 1987).
- 967 42. Marco, S., Agnon, A., Ellenblum, R. & Eidelman, A. 817-year-old walls offset
968 sinistrally 2.1 m by the Dead Sea Transform, Israel. *Journal of Geodynamics* **24**,
969 11–20 (1997).
- 970 43. Ellenblum, R., Marco, S., Agnon, A. & Rockwell, T. Crusader castle torn apart by

971 earthquake at dawn, 20 May 1202. *Geology* **26**, 303–306 (1998).

972 44. Daeron, M. *et al.* Sources of the large A.D. 1202 and 1759 Near East earthquakes.

973 *Geology* **33**, 529–8 (2005).

974 45. Nemer, T., Meghraoui, M. & Khair, K. The Rachaya-Serghaya fault system

975 (Lebanon): Evidence of coseismic ruptures, and the AD 1759 earthquake

976 sequence. *J. Geophys. Res.* **113**, 61–12 (2008).

977 46. Gomez, F. *et al.* Coseismic displacements along the Serghaya Fault: an active

978 branch of the Dead Sea Fault System in Syria and Lebanon. *Journal of the*

979 *Geological Society* **158**, 405–408 (2001).

980 47. Gomez, F., Meghraoui, M. & Darkal, A. N. Holocene faulting and earthquake

981 recurrence along the Serghaya branch of the Dead Sea fault system in Syria and

982 Lebanon. *Geophys. J. Int.* **153**, 658–674 (2003).

983 48. Daeron, M. *et al.* 12,000-Year-Long Record of 10 to 13 Paleoearthquakes on the

984 Yammouneh Fault, Levant Fault System, Lebanon. *Bulletin of the Seismological*

985 *Society of America* **97**, 749–771 (2007).

986 49. Elias, A. *et al.* Active thrusting offshore Mount Lebanon: Source of the

987 tsunamigenic A.D. 551 Beirut-Tripoli earthquake. *Geology* **35**, 755–4 (2007).

988 50. Ellenblum, R. *et al.* Archaeological record of earthquake ruptures in Tell Ateret,

989 the Dead Sea Fault. *Tectonics* **34**, 2105–2117 (2015).

990 51. Nemer, T. & Meghraoui, M. Evidence of coseismic ruptures along the Roum fault

991 (Lebanon): a possible source for the AD 1837 earthquake. *Journal of Structural*

992 *Geology* **28**, 1483–1495 (2006).

993 52. Biasi, G. P. & Wesnousky, S. G. Steps and Gaps in Ground Ruptures: Empirical

994 Bounds on Rupture Propagation. *Bulletin of the Seismological Society of America*

995 **106**, 1110–1124 (2016).

996 53. Savage, J. C. Empirical earthquake probabilities from observed recurrence

997 intervals. *Bulletin of the Seismological Society of America* **84**, 219–221 (1994).

998 54. Biasi, G. P., Weldon, R. J. & Fumal, T. E. Paleoseismic event dating and the

999 conditional probability of large earthquakes on the southern San Andreas fault,

1000 California. *Bulletin of the Seismological Society of America* **92**, 2761–2781 (2002).

1001 55. Reimer, P. J. *et al.* IntCal13 and Marine13 Radiocarbon Age Calibration Curves 0–

1002 50,000 Years cal BP. *Radiocarbon* **55**, 1869–1887 (2013).

1003 56. Stuiver, M. & Polach, H. A. Discussion Reporting of ¹⁴C data. *Radiocarbon* **19**, 355–

1004 363 (1977).

1005

1006

1007

1008

1009

1010

1011

1012

1013

1014

1015

1016

1017

1018

1019

1020 8. Table and figures

1021

| Sample name | Laboratory Code | Fraction Modern | ± | δ ¹⁴ C (‰) | ± | ¹⁴ C age (BP) | ± | modeled calibrated age(±2σ) |
|-------------|-----------------|-----------------|--------|-----------------------|-----|--------------------------|-----|-----------------------------|
| TAY14-02 | UCIAMS 164533 | 0.8592 | 0.0012 | -140.8 | 1.2 | 1220 | 15 | 718 - 878 |
| TAY14-11 | UCIAMS 164534 | 0.7652 | 0.0011 | -234.8 | 1.1 | 2150 | 15 | 145 BC - 61 BC |
| TAY14-9 | UCIAMS 158597 | 0.9486 | 0.0017 | -51.4 | 1.7 | 425 | 15 | 1436 - 1475 |
| TAY14-17 | UCIAMS 164535 | 0.4071 | 0.0058 | -592.9 | 5.8 | 7220 | 120 | 6256 BC - 5759 BC |
| TAY14-30 | UCIAMS 158598 | 0.613 | 0.0009 | -387 | 0.9 | 3930 | 15 | 2477 BC - 2347 BC |
| TAY14-37 | UCIAMS 158599 | 0.6899 | 0.0021 | -310.1 | 2.1 | 2980 | 25 | 1277 BC - 1121 BC* |
| TAY14-38 | UCIAMS 158600 | 0.7587 | 0.001 | -241.3 | 1.0 | 2220 | 15 | 362 BC - 205 BC |
| TAY14-41 | UCIAMS 158601 | 0.5208 | 0.004 | -479.2 | 4.0 | 5240 | 70 | 4247 BC - 3820 BC |
| TAY14-42 | UCIAMS 158602 | 0.366 | 0.0008 | -634 | 0.8 | 8075 | 20 | 7079 BC - 7041 BC |
| TAY14-43 | UCIAMS 158603 | 0.4878 | 0.0008 | -512.2 | 0.8 | 5765 | 15 | 4685 BC - 4552 BC |
| TAY14-44 | UCIAMS 158604 | 0.9328 | 0.0013 | -67.2 | 1.3 | 560 | 15 | 1319 - 1415 |
| TAY14-51 | UCIAMS 158605 | 0.4478 | 0.0008 | -552.2 | 0.8 | 6455 | 15 | 5476 BC - 5376 BC |
| TAY14-54 | UCIAMS 158606 | 0.7799 | 0.0011 | -220.1 | 1.1 | 1995 | 15 | 164 BC - 81 BC |
| TAY14-55 | UCIAMS 158607 | 0.7933 | 0.0011 | -206.7 | 1.1 | 1860 | 15 | 90 - 228 |
| TAY14-56 | UCIAMS 158608 | 0.9741 | 0.0017 | -25.9 | 1.7 | 210 | 15 | 1765 - 1953 |
| TAY14-58 | UCIAMS 158609 | 0.7756 | 0.0011 | -224.4 | 1.1 | 2040 | 15 | 100 BC - 4 AD |
| TAY14-59 | UCIAMS 158610 | 0.7293 | 0.0012 | -270.7 | 1.2 | 2535 | 15 | 910 BC - 833 BC |
| TAY14-60 | UCIAMS 158611 | 0.6277 | 0.001 | -372.3 | 1.0 | 3740 | 15 | 2202 BC - 2050 BC* |
| TAY14-61 | UCIAMS 158612 | 0.9777 | 0.0019 | -22.3 | 1.9 | 180 | 20 | 1774 - 1953 |
| TAY14-63 | UCIAMS 158613 | 0.7541 | 0.0011 | -245.9 | 1.1 | 2270 | 15 | 381 BC - 232 BC |
| TAY14-65 | UCIAMS 158614 | 0.7385 | 0.0011 | -261.5 | 1.1 | 2435 | 15 | 731 BC - 413 BC |
| TAY14-66 | UCIAMS 158615 | 0.7562 | 0.0011 | -243.8 | 1.1 | 2245 | 15 | 391 BC - 258 BC |
| TAY14-69 | UCIAMS 158616 | 0.9824 | 0.0014 | -17.6 | 1.4 | 145 | 15 | 1666 - 1809 |
| TAY14-70 | UCIAMS 164536 | 0.9825 | 0.0014 | -17.5 | 1.4 | 140 | 15 | 1677 - 1875 |
| TAY14-71 | UCIAMS 164537 | 0.7583 | 0.0011 | -241.7 | 1.1 | 2220 | 15 | 365 BC - 206 BC* |
| TAY14-73 | UCIAMS 158617 | 0.742 | 0.0029 | -258 | 2.9 | 2400 | 35 | 741 BC - 398 BC |
| TAY14-74 | UCIAMS 158618 | 0.7683 | 0.0012 | -231.7 | 1.2 | 2115 | 15 | 147 BC - 56 BC |
| TAY14-75 | UCIAMS 158619 | 0.7074 | 0.001 | -292.6 | 1.0 | 2780 | 15 | 994 BC - 894 BC |
| TAY14-79 | UCIAMS 164538 | 0.8618 | 0.0013 | -138.2 | 1.3 | 1195 | 15 | 774 - 881* |
| TAY14-100 | UCIAMS 158620 | 0.3684 | 0.0007 | -631.6 | 0.7 | 8020 | 20 | 7058 BC - 6830 BC |
| TAY14-119 | UCIAMS 164539 | 0.8045 | 0.0014 | -195.5 | 1.4 | 1750 | 15 | 242 - 337 |
| TAY14-123 | UCIAMS 158621 | 0.7592 | 0.0012 | -240.8 | 1.2 | 2215 | 15 | 361 BC - 258 BC |

1022

1023 Table S1 : Mass Spectroscopy measurements were made at the Keck carbon cycle mass
 1024 spectroscopy facility at University of California, Irvine. Ages were calibrated using OxCal
 1025 4.2⁶ and calibration curve INTCAL13⁵⁵. Calibrated ages are given in date Before Christ
 1026 (BC) or After Christ (AD). Radiocarbon concentrations are given as fractions of the

1027 Modern standard, D14C, and conventional radiocarbon age, following the conventions of
1028 Stuiver and Polach⁵⁶. Sample preparation backgrounds have been subtracted, based on
1029 measurements of ¹⁴C-free wood. All results have been corrected for isotopic
1030 fractionation according to the conventions of Stuiver and Polach⁵⁶, with $\delta^{13}\text{C}$ values
1031 measured on prepared graphite using the AMS spectrometer. These can differ from δ
1032 ¹³C of the original material, if fractionation occurred during sample graphitization or the
1033 AMS measurement, and are not shown.

1034 * Samples that are out of stratigraphic order, most probably reworked. They are not
1035 included in the age model.

1036
1037
1038



1039
1040
1041

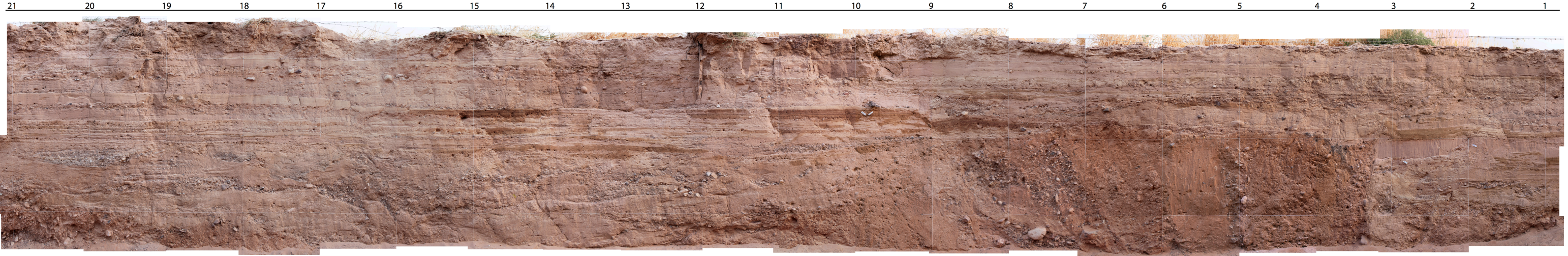
1042 Figure S1: Field view of the alluvial fan of the Wadi Musa. The picture is taken from the
1043 uplifted fan, the trenching place is visible on the active fan, as well as a small pressure
1044 ridge (~60cm high).

1045
1046
1047
1048
1049
1050
1051
1052
1053
1054
1055

1056
1057 Figure S2: Photomosaic of the trench southern wall (top) and mapping of stratigraphic
1058 layers, faults, and earthquakes (bottom). The event horizons associated to the seismic
1059 events recorded in the trench are indicated in red on the stratigraphic log.

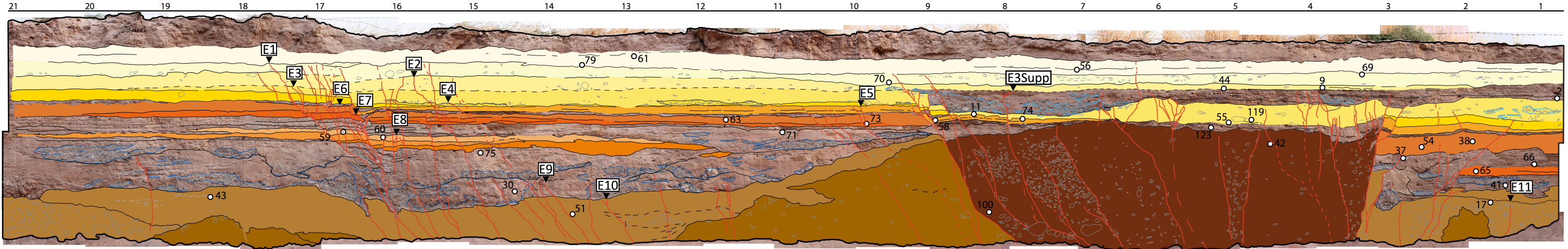
East

West



East

West



1m

fault ¹⁴C sample
 E1 event horizon

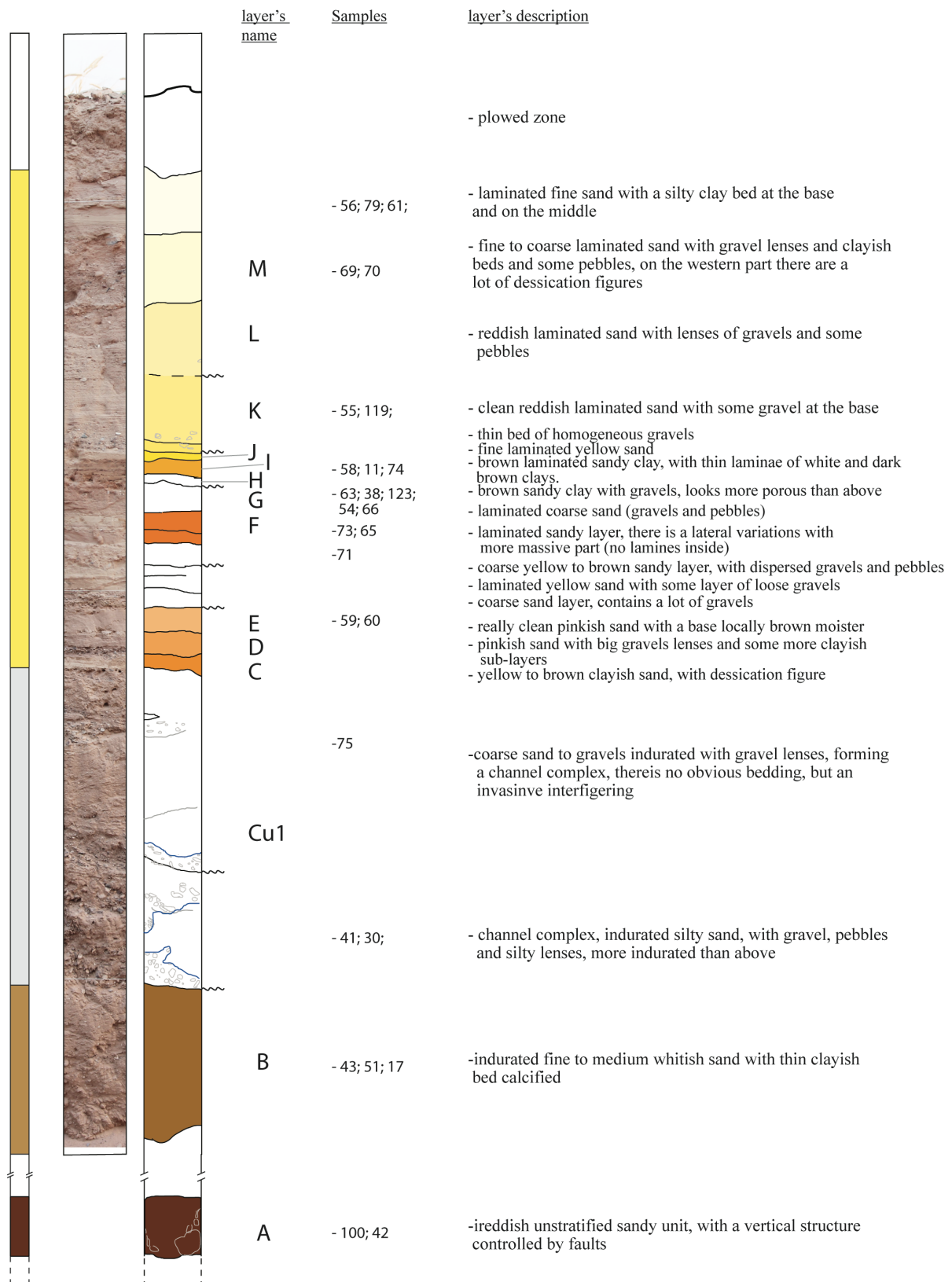
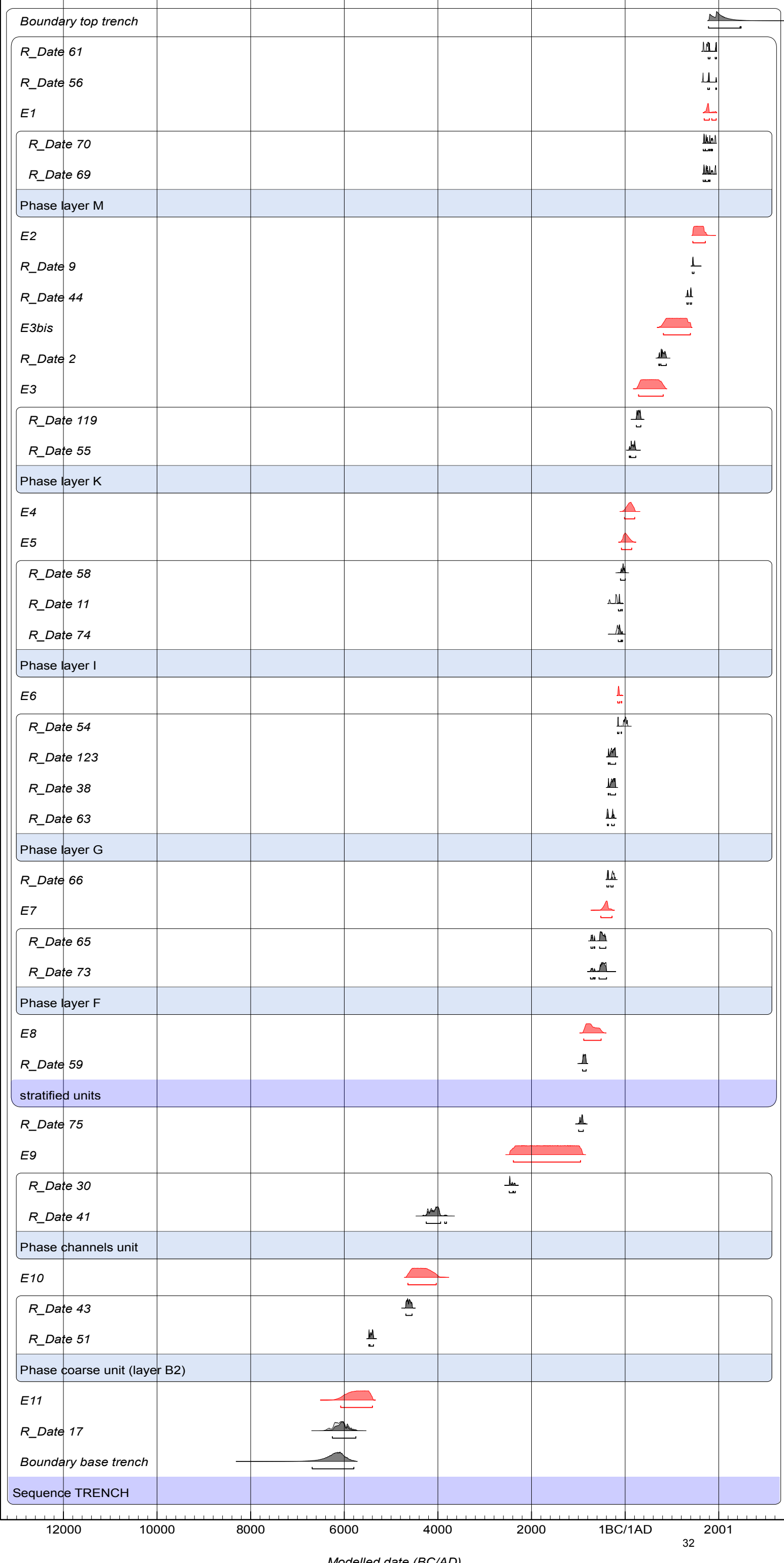


Figure S3: Stratigraphic log of the trench, on the left simplified log with the limits of the four main units, and then the complete log is represented. Letters A to M names the different stratigraphic layers. The layers are quite continuous laterally along the trench, the ¹⁴C samples dated in each layer are indicated.

Figure S4: Age model computed for the trench stratigraphy using OxCal v4.2⁶ and IntCal13 calibration curve⁵⁴. Dark grey indicates modeled ages including stratigraphic information and red are the modeled age for seismic events. Phases indicate subsets of samples where no stratigraphic order is imposed.



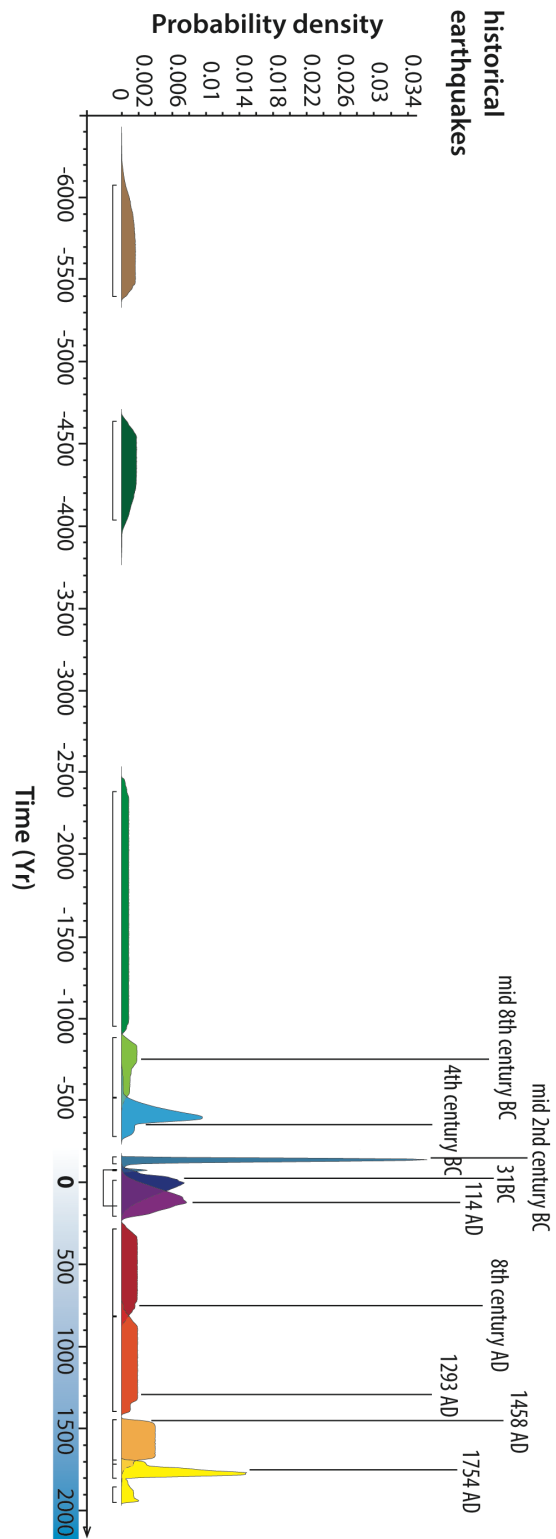


Figure S5: Computed age model from OxCal v4.2⁶ for the seismic events recorded in the trench. The period highlighted in blue corresponds to the times for which we expect that the historical earthquakes record is relatively complete.

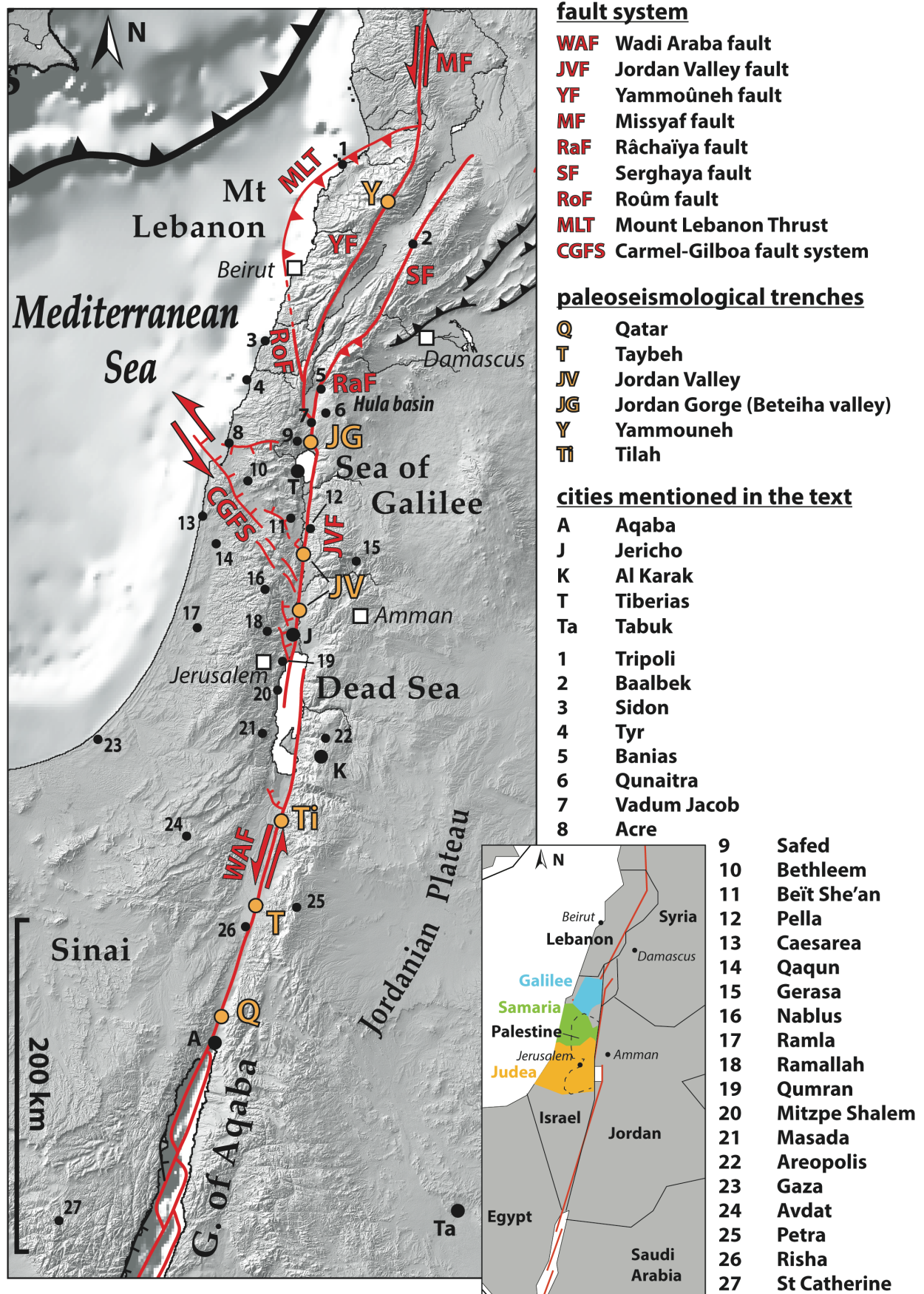


Figure S6: Topographic map of the studied area from SRTM3, faults geometries are derived from Klinger et al.¹⁵. The locations mentioned in the text are reported on the map. The inset map presents the geographical areas mentioned in the text. Figure was generated with Adobe illustrator CS6 (<http://www.adobe.com/fr/products/illustrator.html>)

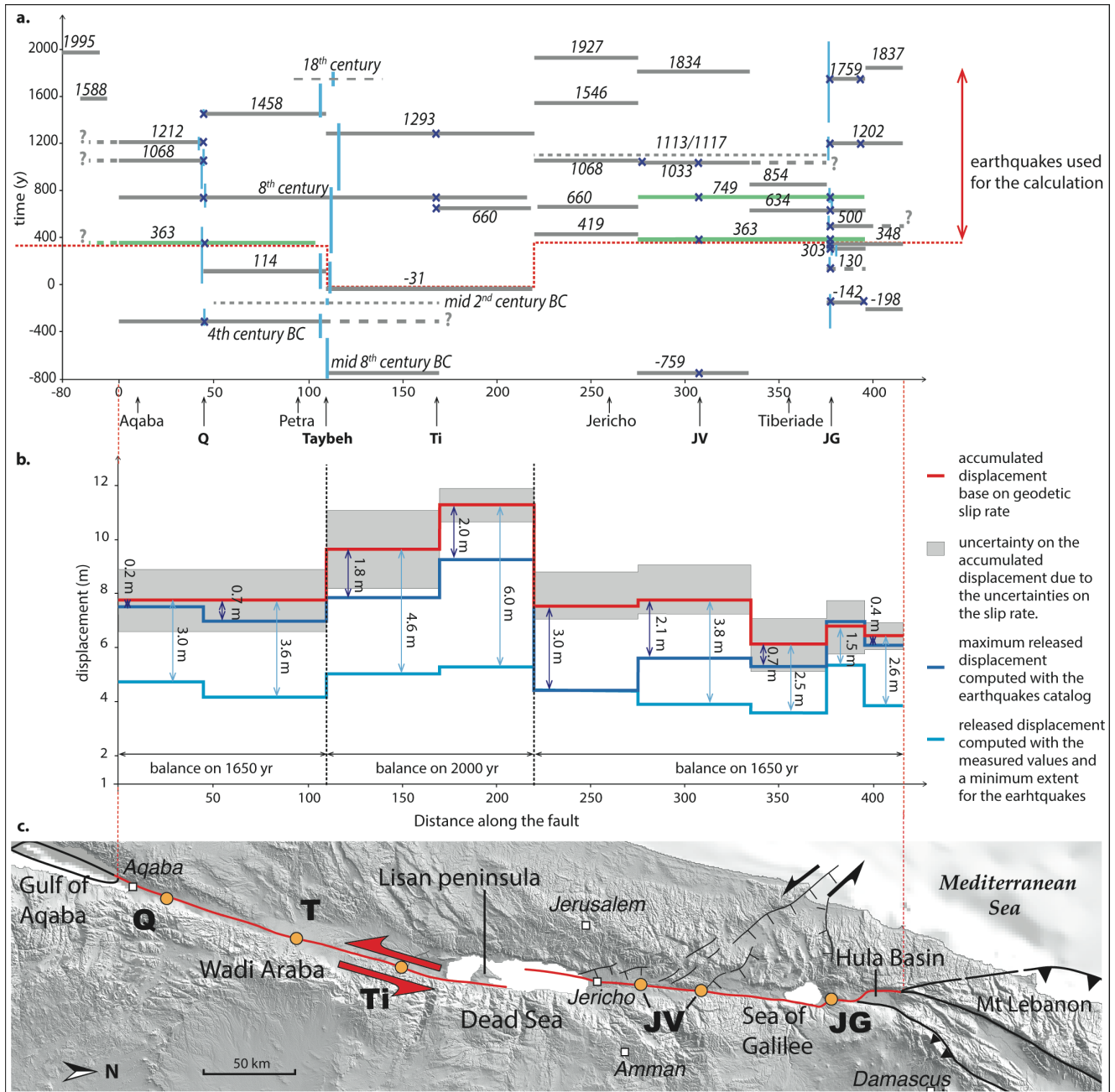


Figure S7: alternative earthquake catalogue for the Dead Sea fault, we consider a longer extent for the two 363 AD events and the 749 AD event. **a.** Historical earthquakes distribution in space and time, each horizontal bar corresponds to an approximate earthquake location along the Dead Sea fault, dashed lines are used for uncertain locations or lateral limits. The vertical bars correspond to the time interval associated to the paleoseismicity at Taybeh, obtained after a Bayesian modeling in Oxcal. For Qatar the time intervals are from Klinger et al.¹⁵, for the Jordan Gorge the ages are from Marco et al.²³ and from Wechsler et al.²¹. The blue crosses represent the earthquakes visible in the different trenches. **b.** Accumulated displacement (red) from tectonic loading and accumulated released slip (blue) due to major earthquakes from 350 AD to 2015 AD along DSF, between the Gulf of Aqaba and the Hula basin. For all earthquakes two

scenarios are considered, the dark blue line shows the released displacement linked to a maximum lateral extent, the light blue line shows the released displacement linked to a minimum lateral extent. The slip deficit is written in meter for all the sections and for the two scenarios. **c.** Simplified structural map of the southern Dead Sea fault, the studied branches are highlighted in red, the sites of previous paleoseismological studies in the area are shown, Q: Qatar, Ti: Tilah, JV: Jordan valley. The topography is from SRTM3 and the faults geometries are derived from Le Béon et al.¹⁵. Figure was generated with Adobe illustrator CS6 (<http://www.adobe.com/fr/products/illustrator.html>)

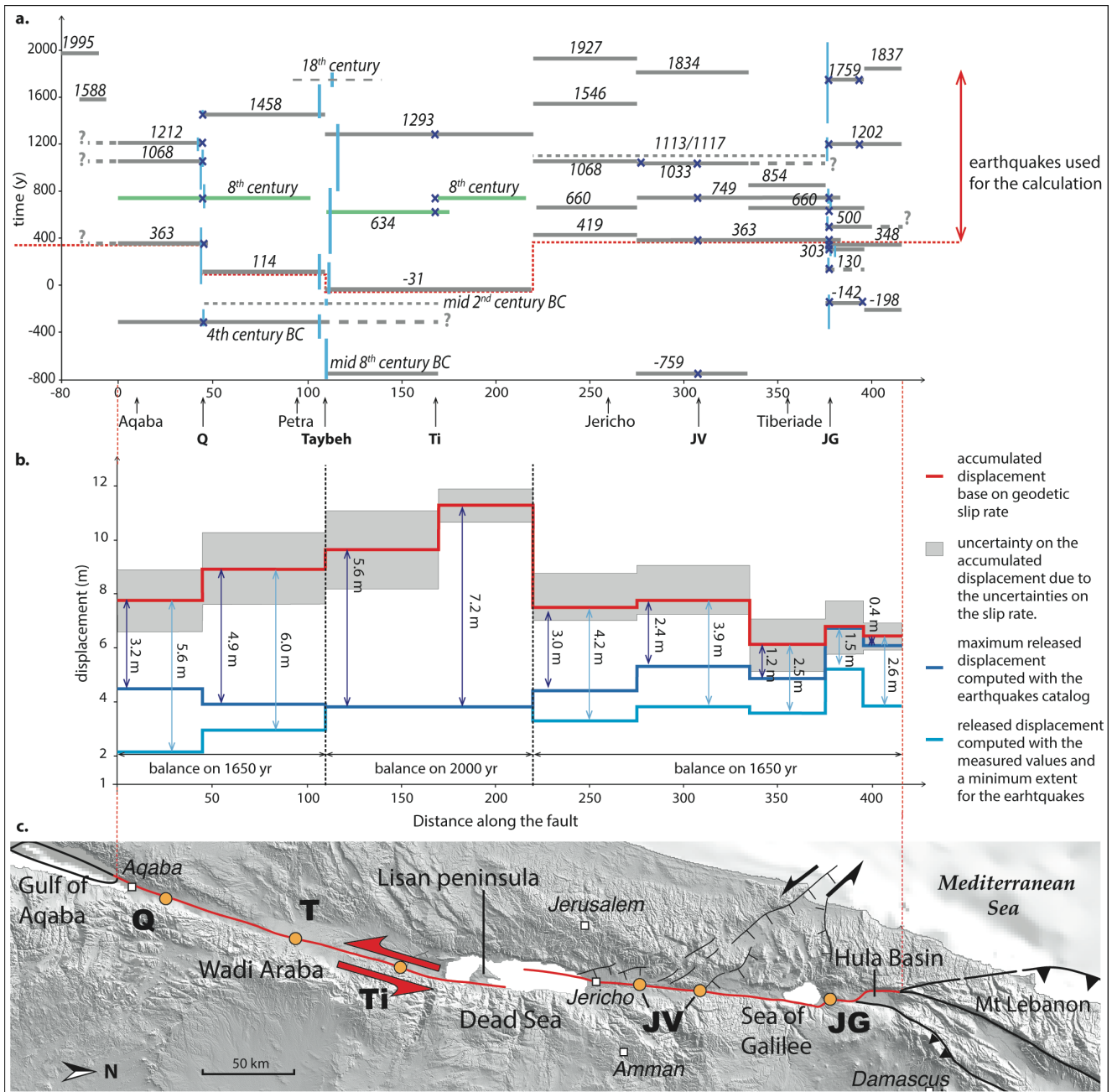


Figure S8: Same as figure S7; here the alternative scenario considers different locations for the 7th and 8th century AD events in the Wadi Araba.

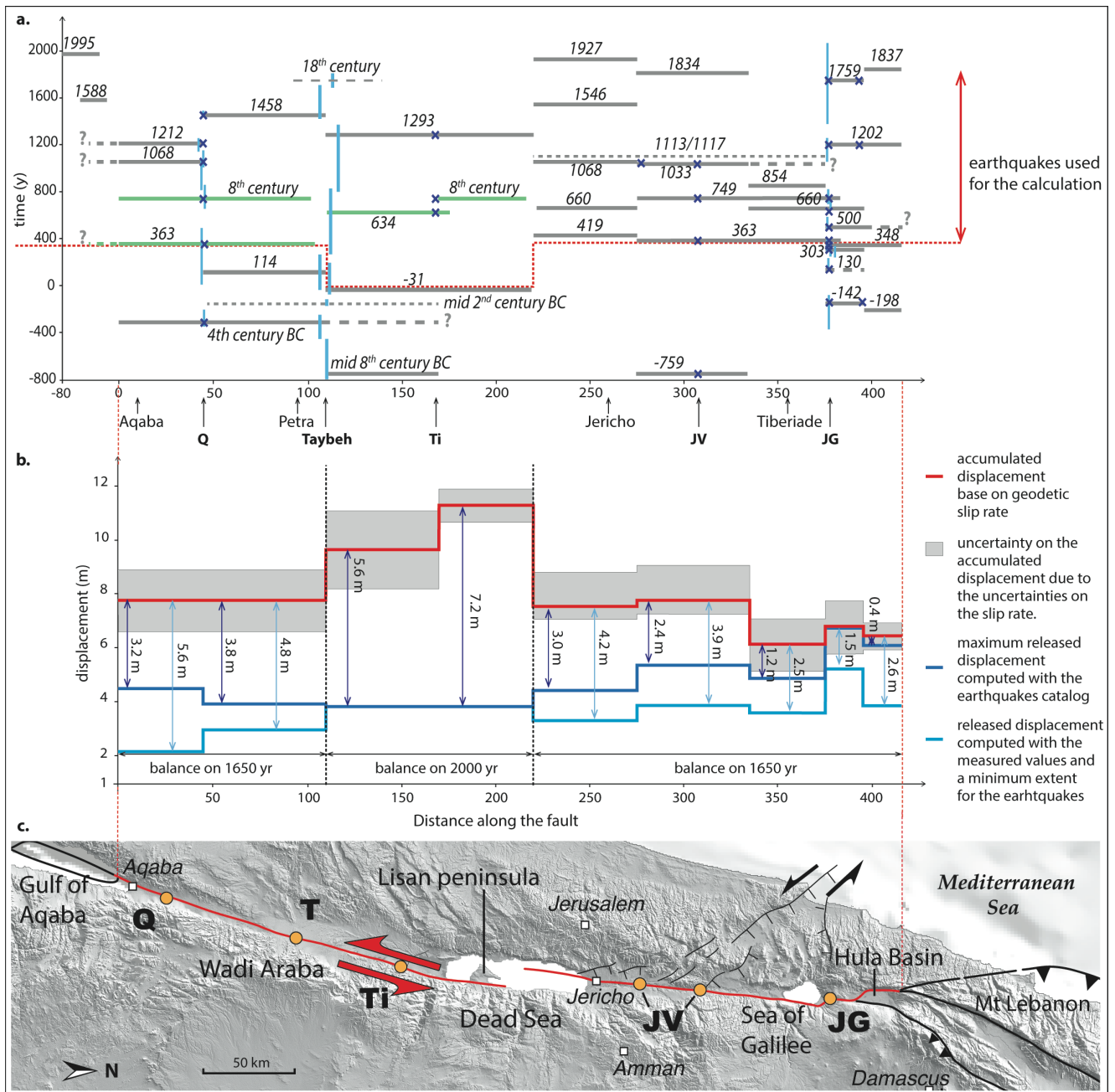


Figure S9: Same as figure S7; here the alternative scenario considers different locations for the 7th and 8th century AD earthquakes in the Wadi Araba, and a larger extension for the 363 AD earthquake.

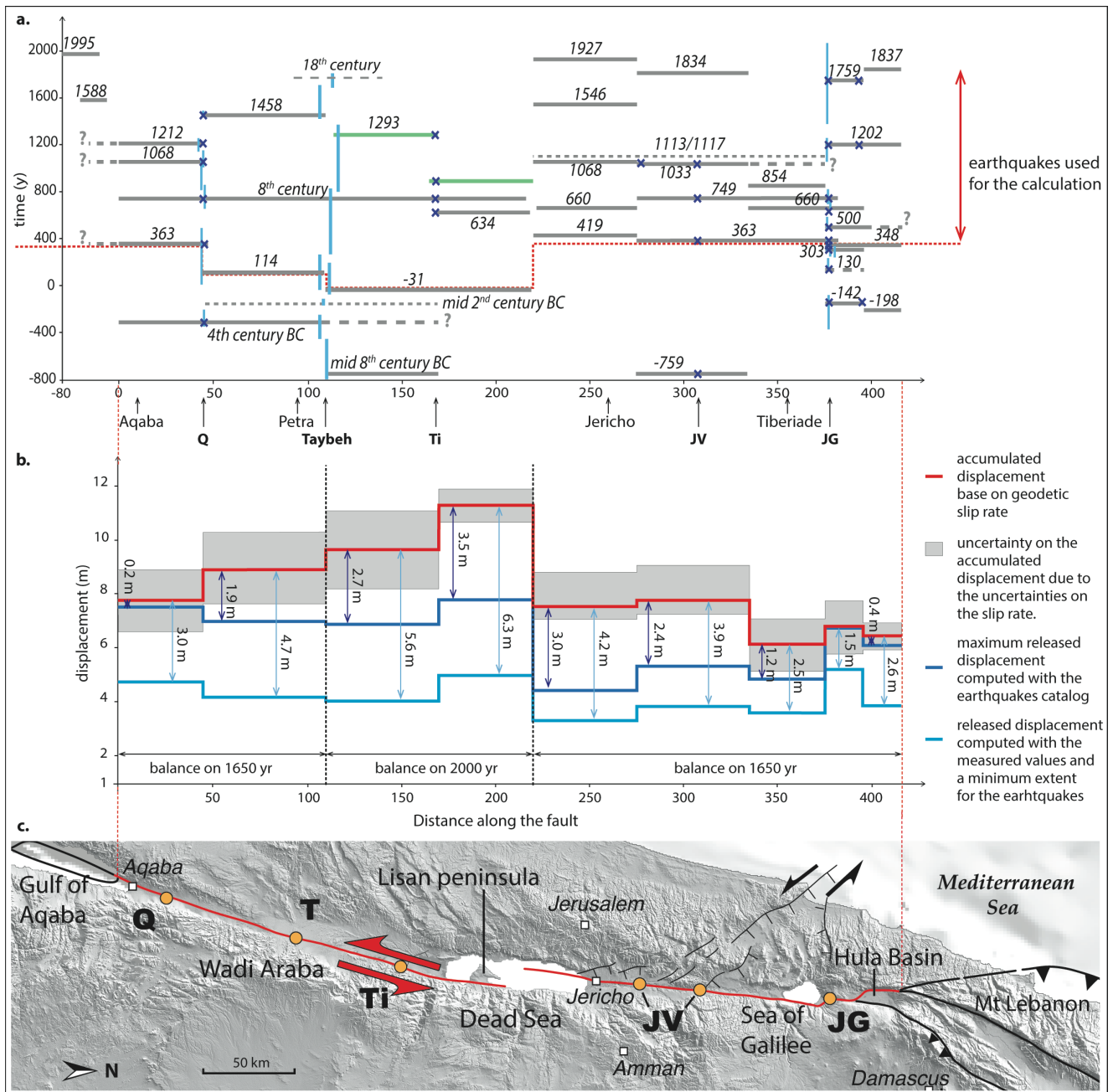


Figure S10: Same as figure S7; here the alternative scenario presents the effect of a smaller 1293 AD earthquake.

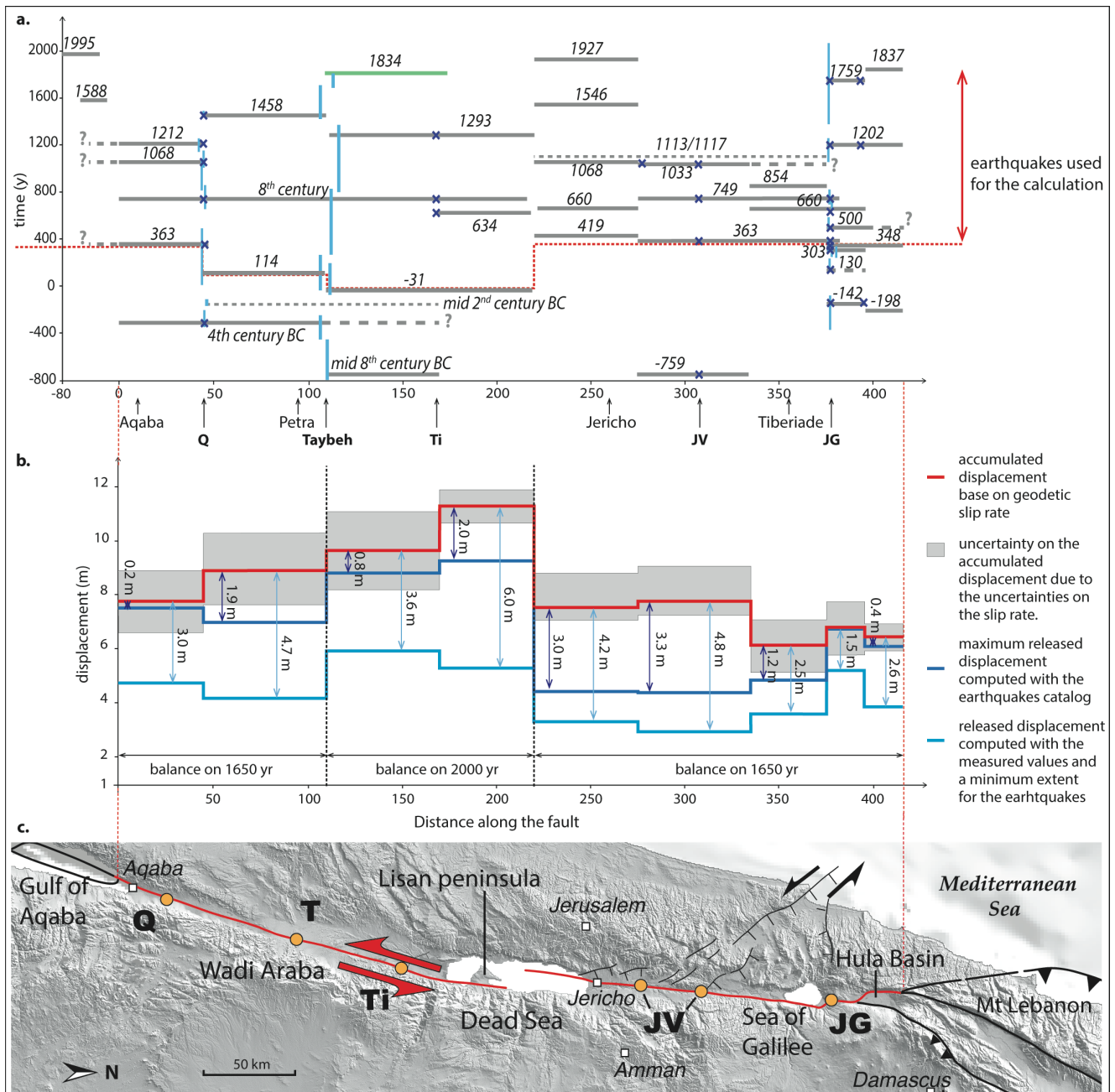


Figure S11: Same as figure S7; here the alternative scenario considers a different location for the 1834 AD earthquake.

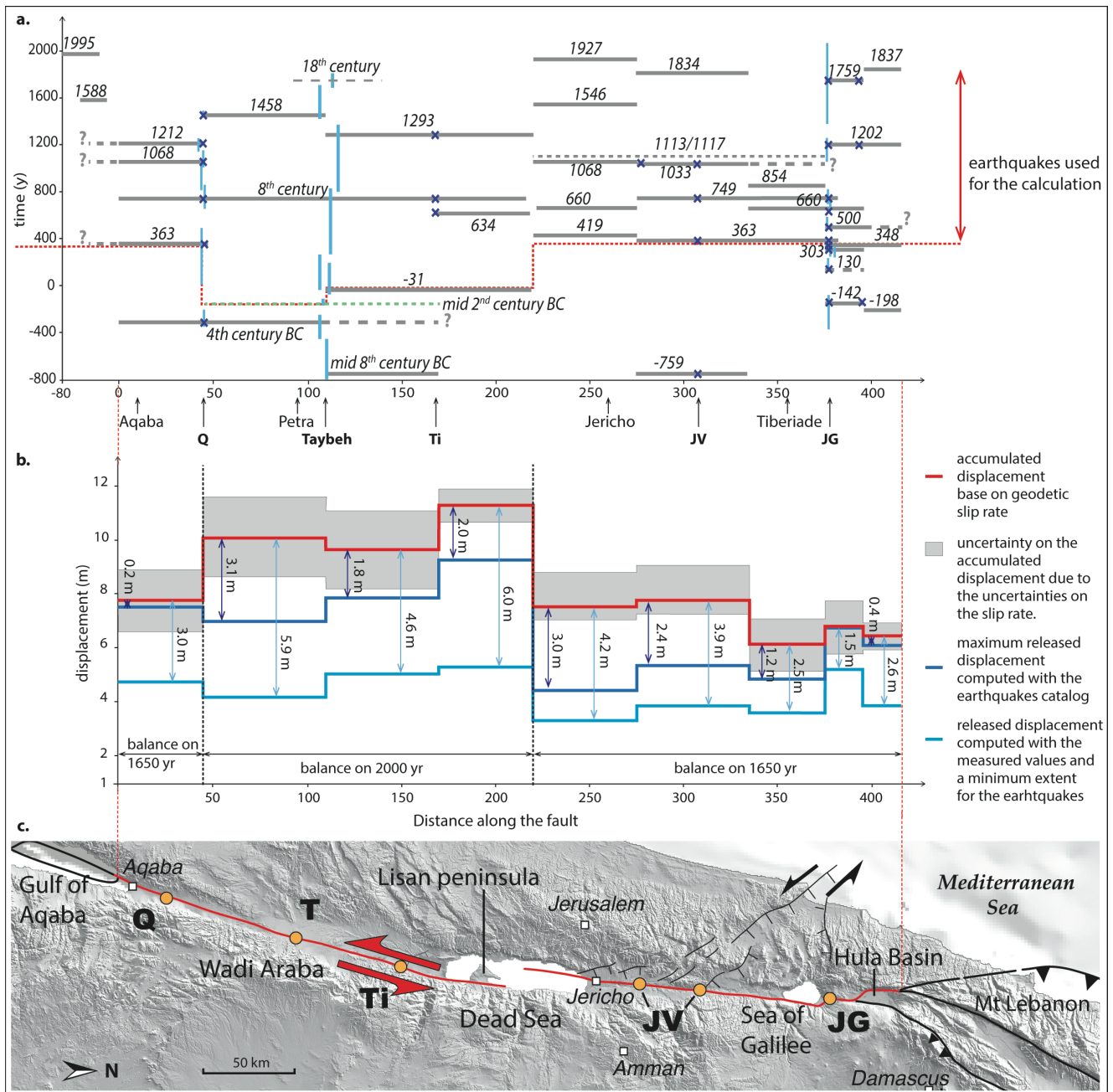


Figure S12: Same as figure S7; here we present an alternative scenario, which does not consider that E5 was an independent event, thus the catalogue does not contain the 114 AD earthquake.